Article

Cell Reports

Coelomocytes Regulate Starvation-Induced Fat Catabolism and Lifespan Extension through the Lipase LIPL-5 in *Caenorhabditis elegans*

Graphical Abstract

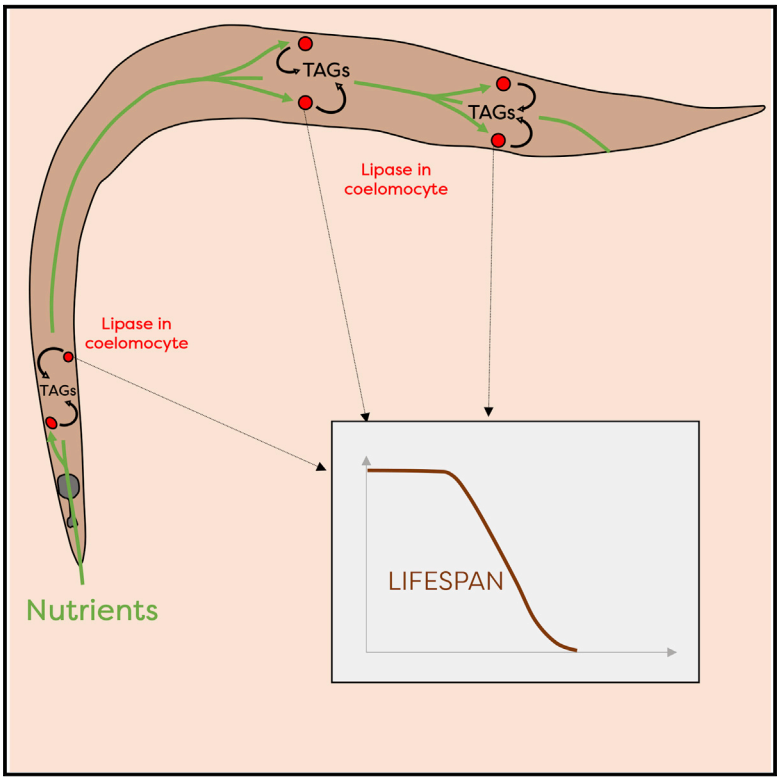

Authors

Alexia Buis, Stéphanie Bellemin, Jérôme Goudeau, Léa Monnier, Nicolas Loiseau, Hervé Guillou, Hugo Aguilaniu

Correspondence

haguilaniu@gmail.com

In Brief

Buis et al. demonstrate that, under conditions of food scarcity, mobilization of triacylglycerides in the gut and lifespan extension of *C. elegans* are regulated by a lipase called LIPL-5 detected exclusively in coelomocytes. The work shows that LIPL-5 links an animal's capacity to withstand nutrient deprivation to fat mobilization.

Highlights

- The lipase LIPL-5 is required for triacylglyceride catabolism under starvation
- LIPL-5 limits lifespan extension under starvation
- LIPL-5 predominantly localizes in coelomocytes
- LIPL-5 controls catabolism and lifespan in coelomocytes

Buis et al., 2019, Cell Reports *28*, 1041–1049
July 23, 2019
https://doi.org/10.1016/j.celrep.2019.06.064

CellPress

Cell Reports
Article

Coelomocytes Regulate Starvation-Induced Fat Catabolism and Lifespan Extension through the Lipase LIPL-5 in *Caenorhabditis elegans*

Alexia Buis,[1,2] Stéphanie Bellemin,[1] Jérôme Goudeau,[1,6] Léa Monnier,[1] Nicolas Loiseau,[3] Hervé Guillou,[3] and Hugo Aguilaniu[1,4,5,7,*]

[1]Institut Génomique Fonctionelle de Lyon/UMR5262, 46 Allee d'Italie, 69364 Lyon Cedex 07, France
[2]Ecole Pratique des Hautes Etudes, Les Patios Saint-Jacques, 4-14 Rue Ferrus, 75014 Paris, France
[3]INRA Toulouse, INRA ToxAlim-Integrative Toxicology & Metabolism-UMR 1331, INRA/INP/UPS, 180 chemin de Tournefeuille-BP 93173, 31027 Toulouse Cedex 3, France
[4]Instituto Serrapilheira, Rua Dias Ferreira 78, Leblon, Rio de Janeiro, Brazil
[5]Detaché from CNRS, Paris, France
[6]Present address: Calico Life Sciences, South San Francisco, CA 94080, USA
[7]Lead Contact
*Correspondence: haguilaniu@gmail.com
https://doi.org/10.1016/j.celrep.2019.06.064

SUMMARY

Dietary restriction is known to extend the lifespan and reduce fat stores in most species tested to date, but the molecular mechanisms linking these events remain unclear. Here, we found that bacterial deprivation of *Caenorhabditis elegans* leads to lifespan extension with concomitant mobilization of fat stores. We find that LIPL-5 expression is induced by starvation and that the LIPL-5 lipase is present in coelomocyte cells and regulates fat catabolism and longevity during the bacterial deprivation response. Either LIPL-5 or coelomocyte deficiency prevents the rapid mobilization of intestinal triacylglycerol and enhanced lifespan extension in response to bacterial deprivation, whereas the combination of both defects has no additional or synergistic effect. Thus, the capacity to mobilize fat via LIPL-5 is directly linked to an animal's capacity to withstand long-term nutrient deprivation. Our data establish a role for LIPL-5 and coelomocytes in regulating fat consumption and lifespan extension upon DR.

INTRODUCTION

A large body of evidence supports links among dietary restriction (DR), fat metabolism, and longevity in numerous species (Masoro et al., 1982; Hansen et al., 2013). DR, defined as diminished food intake without malnutrition, not only decreases fat stores but also modestly (20%–40%) but significantly extends the lifespan of a range of species (Masoro et al., 1982). The capacity to mobilize fat has been shown to play an important role in the ability of mice to withstand food restriction. Various aspects of fat metabolism have been linked lifespan in various species (Bustos and Partridge, 2017; Gonzalez-Covarrubias, 2013; Schroeder and Brunet, 2015), and in humans, although associations between body mass index and morbidity have been established (Afzal et al., 2016), the nature of the molecular link between fat content and longevity remains largely unknown. Altogether, these data suggest that the way fat is mobilized or used may affect the lifespan of wild-type animals subjected to DR.

Here, we investigated the relationship between DR-induced lifespan extension and fat catabolism in *Caenorhabditis elegans*. To date, lipases, that degrade triacylglycerol were shown to affect longevity, but there is no clear evidence for a role for lipases in DR-mediated longevity. For example, in the nematode *C. elegans*, adipose triglyceride lipase-1 (ATGL-1) activity affects lipid storage during nutrient deprivation but does not affect lifespan (Narbonne and Roy, 2009; Noble et al., 2013; Zhang et al., 2010). In contrast, the lipoprotein lipase LIPL-4 is required for lifespan extension of *C. elegans* through ablation of the germline, but modulation of its activity does not affect fat storage or metabolism (O'Rourke et al., 2013). Similarly, fatty acid desaturation plays a key role in promoting lifespan extension of *C. elegans* via effects on autophagy (Goudeau et al., 2011; Lapierre et al., 2011). Although LIPL-1 and LIPL-3 are induced by starvation and their overexpression increases lifespan under normal nutritional conditions, their effect on lifespan occurs independently of DR (O'Rourke and Ruvkun, 2013).

Here, we have explored this question in detail by analyzing fat catabolism in *C. elegans* subjected to DR via bacterial deprivation. We find that expression of the lipase LIPL-5/LIPF is induced by starvation, and animals carrying a mutation in the gene encoding for the lipase LIPL-5/LIPF show decreased triacylglycerol (TAG) consumption and exhibit enhanced lifespan compared with wild-type animals in response to bacterial deprivation. LIPL-5 is expressed in and/or taken up by coelomocytes, which are known as scavenger cells in the body cavity, and we show that functional coelomocytes contribute to both the enhanced TAG metabolism and the extended lifespan induced by bacterial deprivation. Our data are consistent with the idea that coelomocytes fulfill integrative functions (Fares and Greenwald, 2001) and that LIPL-5 is a link for nutrition, fat catabolism, and lifespan that acts in these cells.

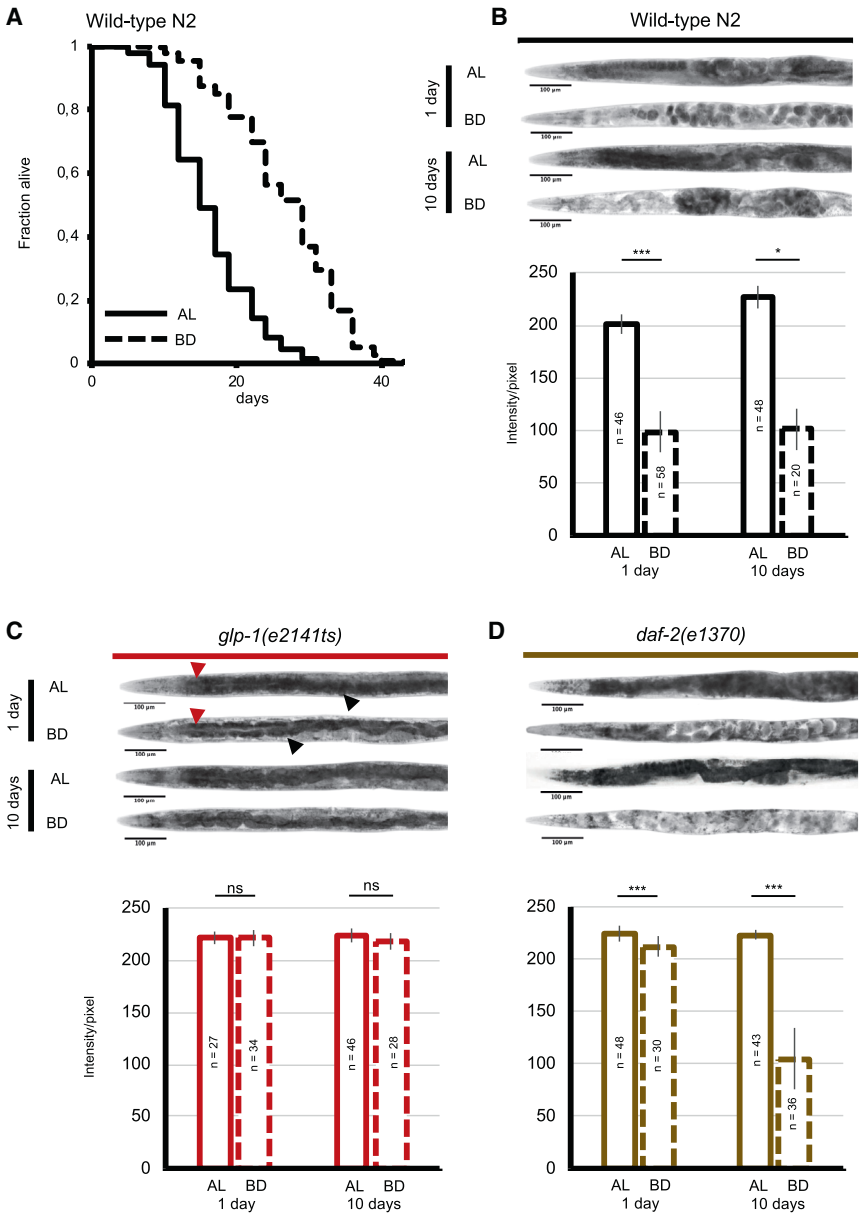

Figure 1. *Caenorhabditis elegans* Loses Fat Stores and Its Lifespan Is Extended upon Bacterial Deprivation

Lifespan analyses of wild-type (N2) *C. elegans* (n > 100 worms) fed *ad libitum* (AL) or subjected to bacterial deprivation. $p < 0.0001$. Mantel-Cox log-rank test. Representative of at least 3 replicate experiments (see Table S2 for number of replicates). Light micrographs of representative oil red O (ORO)-stained whole animals (upper panels) and densitometric quantification of staining of the two first intestinal cells after background removal (lower panels) for the indicated *C. elegans* strains fed AL or subjected to bacterial deprivation (BD) for 1 or 10 days for wild-type animals (A), *glp-1(e2141ts)* mutant animals (B), and *daf-2(e1370)* (D). (C) Red arrows show intestinal fat, while black arrows show hypodermis with or without fat. Mean ± SD of n = at least 20 worms. ns, not significant; $^{**}p < 0.01$ and $^{***}p < 0.001$ by two-tailed Mann-Whitney U test. Representative of 3 biological replicates. See also Figures S1–S3.

RESULTS

Bacterial Deprivation Promotes Fat Consumption and Extends Lifespan

To explore the relationship between fat metabolism and lifespan extension, we measured whole-body TAG fat content and lifespan in animals fed *ad libitum* or subjected to DR for 24 h and until 10 days (Figures 1A and 1B). Although DR can be achieved through various feeding and genetic protocols in *C. elegans* (Greer and Brunet, 2009), we elected to use bacterial deprivation because it is the severest method of DR (Kaeberlein et al., 2006; Sutphin and Kaeberlein, 2008). To test this, we measured TAG content of wild-type animals using oil red O (ORO) staining, Sudan black staining, and thin-layer chromatography (Figures 1B, S1, and S2). We found that animals harbored larger TAG stores than they did under *ad libitum* feeding conditions using ORO staining and thin-layer chromatography (Figures 1B and S1). Using Sudan black staining, we also found wild-type animals lost intestinal TAG, but this difference was at the limit of statistical significance. It reached statistical difference using one statistical test (two-tailed Student's t test), but not another test (two-tailed Mann-Whitney U test) (Figure S1). Altogether, our results are in line with previous observations (Lapierre et al., 2013; O'Rourke et al., 2009). We detected a significant and rapid reduction in fat stores (within 24 h) when animals were subjected to bacterial deprivation (Figure 1B). Long-lived animals such as the germline-less *glp-1(e2141ts)* mutants or the *daf-2(e1370)* mutants, which have defective insulin-insulin growth factor 1 (IGF-1)-like receptor signaling, have larger TAG stores than wild-type animals when fed *ad libitum*, and they consume them at a slower pace when subjected to DR (Figures 1C and 1D). Altogether, these data suggest that the consumption of fat stores is associated with lifespan and may therefore alter the effect of DR on longevity. We therefore searched for enzymes capable of affecting fat stores during bacterial deprivation.

LIPL-5 Mediates Triacylglyceride Catabolism in Adult *C. elegans*

TAG is catabolized to free fatty acids and glycerol by the action of lipases. Five lipase genes (*lipl-1–lipl-5*) are known to be rapidly and transiently induced by DR in *C. elegans* (O'Rourke and Ruvkun, 2013), which is consistent with the observation that

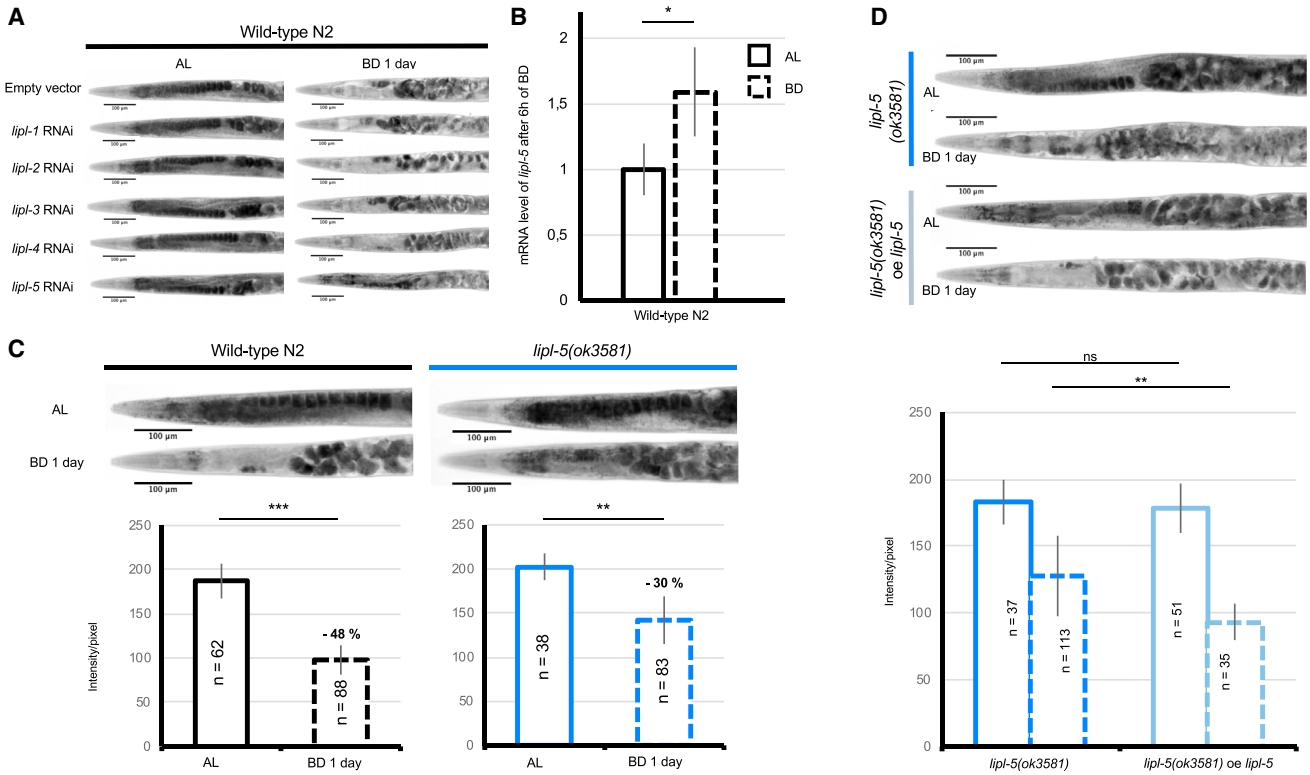

Figure 2. LIPL-5/LIPF Mediates Fat Catabolism Induced by Bacterial Deprivation

(A) Oil red O (ORO) staining of fat stores in wild-type *C. elegans* subjected to *lipl-1*, *lipl-2*, *lipl-3*, *lipl-4*, or *lipl-5* RNAi. Animals were fed *ad libitum* (AL) or subjected to bacterial deprivation (BD) for 1 day.

(B) qRT-PCR analysis of *lipl-5* mRNA in wild-type *C. elegans* subjected to BD for 6 h. Representative of 3 biological replicates. Mean ± SD of n > 20 worms. *p < 0.05 by Student's t test.

(C) Light micrographs of representative oil red O (ORO)-stained whole animals (upper panels) and densitometric quantification of staining of the two first intestinal cells after background removal (lower panels) for wild-type *C. elegans* and *lipl-5(ok3581)* mutants fed AL or subjected to BD for 1 day. Mean ± SD of n > 20 worms. **p < 0.01 and ***p < 0.001 by two-tailed Mann-Whitney U test. Representative of 6 biological replicates.

(D) Light micrographs of representative oil red O (ORO)-stained whole animals (upper panels) and densitometric quantification of staining of the two first intestinal cells after background removal (lower panels) for *lipl-5(ok3581)* either expressing an empty vector or expressing *lipl-5* (expression drive by its endogenous promoter) fed AL or subjected to BD for 1 day. Solid bars, BD; dashed bars, AL. Mean ± SD of n = at least 20 worms. ns, not significant; **p < 0.01 by two-tailed Mann-Whitney U test. Representative of 3 biological replicates.

See also Figures S4 and S5.

wild-type animals consume most of their TAG stores within 24 h of bacterial deprivation (Figure 1B) (McKay et al., 2003). To test the involvement of these enzymes in bacterial deprivation-induced fat catabolism in fertile adults, we inactivated each gene using RNAi. We found that RNAi efficiently suppressed all genes except *lipl-4* (Figure S3A). The relative inefficiency of *lipl-4* RNAi may be because of the particularly strong induction of this enzyme by bacterial deprivation (data not shown). However, because *lipl-4*(*tm4417*) mutants contain normal TAG levels under *ad libitum* and DR conditions (O'Rourke et al., 2009), we considered LIPL-4 unlikely to be relevant to our investigation. Only *lipl-5* inactivation by RNAi in fertile wild-type *C. elegans* reduced TAG catabolism (Figures 2A and S3B). LIPL-5 is highly homologous to isoform 1 of the human gastric triacylglycerol lipase LIPF. Thus, we confirmed that *lipl-5* is induced by nutrient shortage (Figure 2B) and its inhibition prevents TAG catabolism upon bacterial deprivation (Figure 2A). The induction of *lipl-5* we measured was robust but modest and transient; we detected significant induction after 6 h (Figure 2B), but this induction failed to reach statistical significance after 12 h (data not shown). These results confirmed data previously published by the Ruvkun lab (O'Rourke et al., 2009). To confirm the results obtained with *lipl-5* RNAi data, we examined *lipl-5(ok3581)* mutants, which carry a 300 bp deletion in the *lipl-5* gene. These animals exhibited an inability to catabolize fat similar to that of wild-type animals subjected to *lipl-5* RNAi (Figure 2C). We also generated an independent *lipl-5(bab-8)* deletion strain by CRISPR/Cas9-mediated editing (MCP12), which showed a similarly reduced capacity to catabolize fat upon bacterial deprivation (Figure S4). Finally, overexpression of *lipl-5* under the control of the endogenous *lipl-5* promoter was sufficient to increase fat catabolism in *lipl-5(ok3581)* mutants upon bacterial deprivation (Figure 2C). These data establish a central role for LIPL-5 in bacterial deprivation-induced fat catabolism in *C. elegans*.

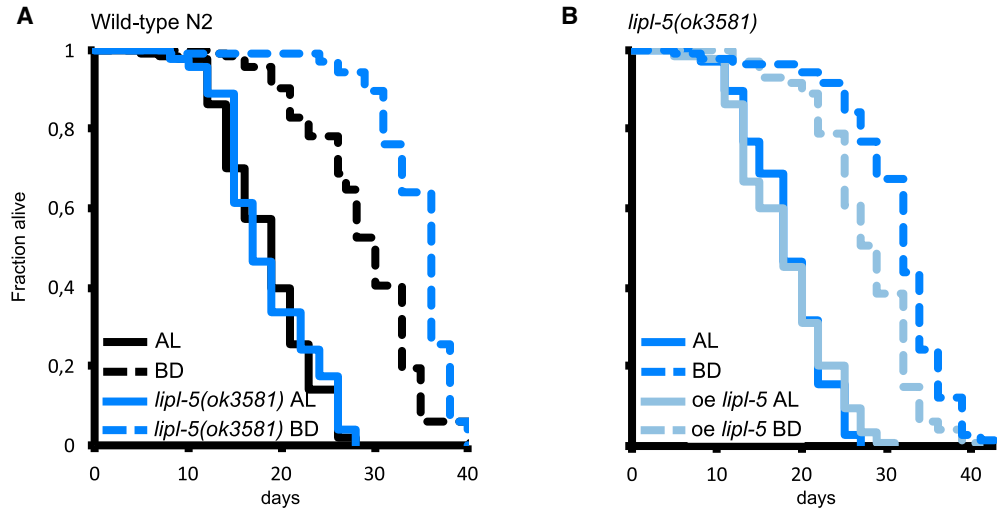

Figure 3. LIPL-5/LIPF Limits Lifespan Extension in Response to Bacterial Deprivation

Lifespan analyses of *C. elegans* fed *ad libitum* (AL) or subjected to bacterial deprivation (BD).

(A) BD extended lifespan by 56% for wild-type animals ($p < 0.0001$) and 86% for *lipl-5(ok3581)* mutant animals ($p < 0.0001$). The mean lifespan of wild-type animals was similar to that of *lipl-5(ok3581)* mutant animals in similar conditions ($p = 0.515$). In BD, the lifespan of wild-type animals was 16% lower than that of *lipl-5(ok3581)* mutant animals ($p < 0.001$).

(B) BD extended lifespan by 72% for *lipl-5(ok3581)* mutant animals ($p < 0.0001$) and 50% for *lipl-5(ok3581)* mutant animals overexpressing *lipl-5* behind its own promoter ($p < 0.0001$). The mean lifespan of *lipl-5(ok3581)* mutant animals was similar to that of *lipl-5(ok3581)* mutant animals overexpressing *lipl-5* behind its own promoter in AL ($p = 0.651$). In BD, the lifespan of *lipl-5(ok3581)* mutant animals was 12% higher than that of *lipl-5(ok3581)* mutant animals overexpressing *lipl-5* behind its own promoter ($p < 0.001$). Mean ± SD of n = at least 100 worms. Mantel-Cox log-rank test (see Table S2 for number of replicates).

LIPL-5, Predominantly Localized in Coelomocytes, Limits Bacterial Deprivation-Induced Longevity

Because the *lipl-5(ok3581)* mutants fail to catabolize fat in response to bacterial deprivation, we examined the influence of *lipl-5* deletion and restoration on lifespan extension in response to bacterial deprivation. The *lipl-5(ok3581)* mutants exposed to bacterial deprivation experienced a lifespan extension nearly twice that of wild-type animals (Figure 3A; Table S2), and conversely, re-expression of *lipl-5* in the mutants reversed the bacterial deprivation-extended lifespan to the duration seen with wild-type animals (Figure 3B; Table S2). Altogether, these experiments establish that LIPL-5 regulates both fat catabolism and DR-induced lifespan extension in *C. elegans*.

We next investigated the cellular localization of LIPL-5 in *C. elegans*. To this end, we expressed a fusion protein consisting of LIPL-5 and the fluorescent dye tdTOMATO, which emits light at high wavelengths, allowing ready visualization of LIPL-5 against the relatively high green autofluorescent background exhibited by *C. elegans*. Animals were injected with plasmids containing extrachromosomal arrays of LIPL-5::tdTOMATO under the control of the endogenous promoter, which typically leads to significant overexpression of the protein. LIPL-5::tdTOMATO fluorescence was only detected in the six coelomocytes of *C. elegans* (Figure 4A), which are specialized endocytotic cells of mesodermal origin located in the pseudocoelom (Fares and Greenwald, 2001; Zhang et al., 2001). Coelomocytes are thought to be involved in detoxification and have been proposed to be proto-hepatocytes (Fares and Greenwald, 2001). To ensure that this unexpected finding was not caused by artifactual uptake of supra-physiological levels of LIPL-5::tdTOMATO, we generated additional mutants using CRISPR/Cas9 editing to place a single copy of LIPL-5::tdTOMATO at the endogenous locus. Because some lipases are known to be more potent at acidic pH and are usually lysosomal, we also introduced a lysosome-associated membrane protein 1 (LMP-1)::GFP marker to test for LIPL-5 co-localization in this organelle. We found that LIPL-5 was localized specifically in the lysosomes of coelomocytes, even in the strain expressing physiological levels of the reporter protein (Figures 4B and 4C). To determine whether LIPL-5 is expressed by coelomocytes or produced elsewhere and then endocytosed, we used the intestinal-specific promoter *ges*-1 to enforce LIPL-5 expression in the gut, where lipases are generally abundant. LIPL-5::tdTOMATO was also found predominantly in coelomocytes in these animals (Figure S5A), indicating that LIPL-5 can be transported to or endocytosed by coelomocytes. Gut-specific overexpression of LIPL-5 was able to increase fat catabolism and reduce the enhanced lifespan response to bacterial deprivation exhibited by *lipl-5(ok3581)* mutants, suggesting that coelomocyte-localized LIPL-5 plays an important role in modulating these phenotypes (Figures S5B and S5C).

Coelomocytes Play a Central Role in Regulating Fat Metabolism and Lifespan in *C. elegans*

To test the importance of coelomocytes in the fat catabolism and longevity phenotypes induced by bacterial deprivation, we employed the coelomocyte-deficient strain NP717, which

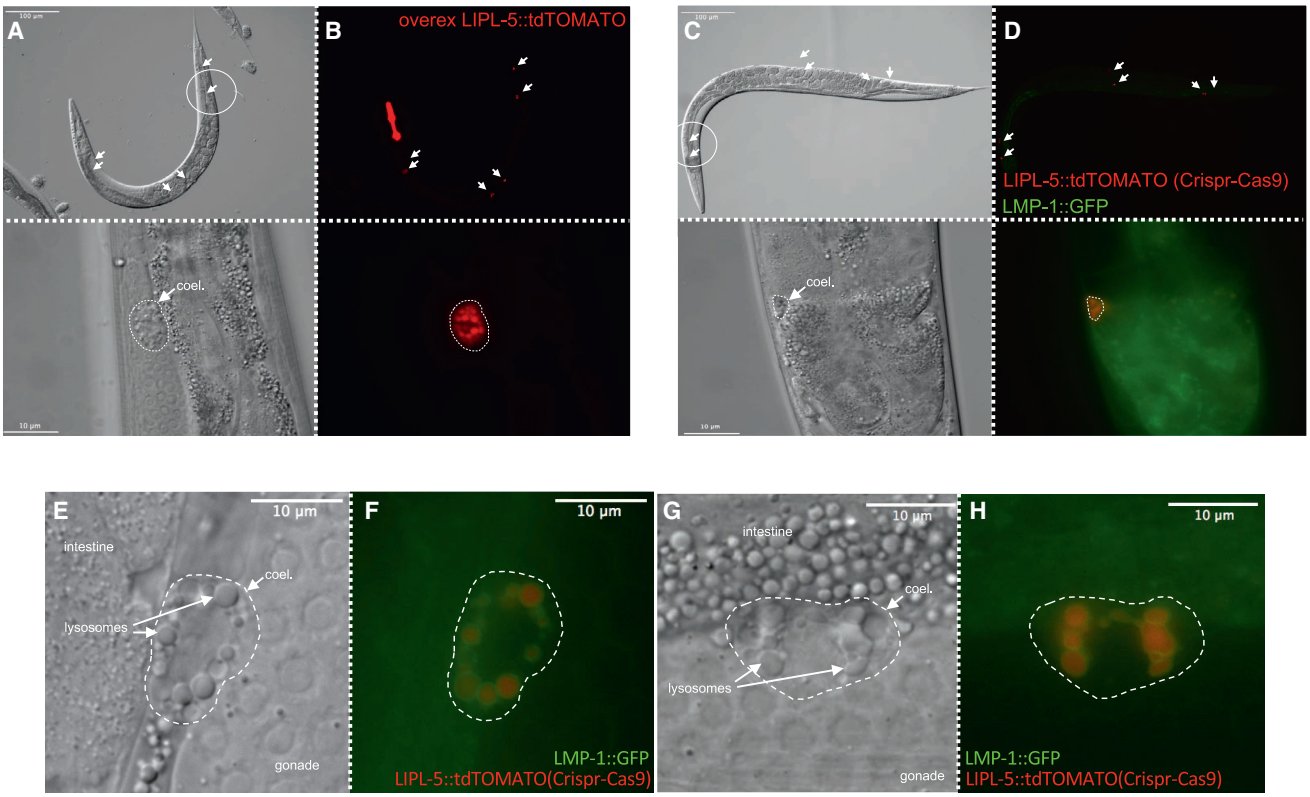

Figure 4. LIPL-5/LIPF Is Localized to Coelomocyte Lysosomes

(A and B) (A) Differential interference contrast images and (B) fluorescence images of adult wild-type *C. elegans* expressing tdTOMATO-tagged LIPL-5 driven by the endogenous promoter. Upper and lower panels show the same animal at different magnifications (scale bars: 100 μm and 10 μm, respectively). The LIPL-5::tdTOMATO signal is confined to coelomocytes (white arrows and dashed circles).

(C and D) (C) Images are as described for (A) and (B) except that (D) animals co-expressed LIPL-5::tdTOMATO and GFP-tagged LMP-1 (lysosome-associated membrane protein) to visualize lysosomes. White arrows and dashed circle indicate coelomocytes.

(E–H) (E and G) Differential interference contrast and (F and H) fluorescence images similar to (A) and (B), respectively, except at a higher magnification to show coelomocytes. Each experiment was replicated at least 3 times (biological replicates).

expresses a variant of the diphtheria toxin A fragment (E148D) under the control of the coelomocyte-specific *unc-122* promoter (Fares and Greenwald, 2001). This strain also expresses GFP fused to a signal sequence from SEL-1, which is expressed in the body wall under the *myo-3* promoter. In normal animals, ssGFP is secreted into the pseudocoelom and is endocytosed by and accumulates in coelomocytes. In coelomocyte-deficient animals, however, ssGFP accumulates in the pseudocoelom, giving rise to the distinctive coelomocyte uptake (cup) phenotype (Figure S6).

As previously described (Park et al., 2015), the NP717 strain had a shorter lifespan than wild-type animals under *ad libitum* feeding conditions (Figure 5A; Table S2); however, in line with our hypothesis that coelomocytes may play an important role in bacterial deprivation-induced fat and longevity phenotypes, NP717 animals showed diminished fat catabolism and enhanced longevity compared with wild-type animals when subjected to bacterial deprivation, similar to the phenotype of *lipl-5* mutants (Figure 5; Table S2). These results are in apparent contradiction with findings that coelomocyte-deficient animals have a normal lifespan when fed *ad libitum* and are unaffected by various DR protocols (Park and Park, 2017). To our knowledge, the only difference between the experimental protocols was our use of *Escherichia coli* strain *ht115* for *ad libitum* feeding, compared with OP50 used by Park and Park (2017); thus, the reason for this discrepancy remains unclear. However, our results with the NP717 strain and *lipl-5(ok3581)* mutants, together with the LIPL-5 localization study, are consistent with a crucial role for coelomocyte-localized LIPL-5 as a mediator of fat catabolism and lifespan extension induced by bacterial deprivation.

To test this directly, we deleted or overexpressed *lipl-5* in the coelomocyte-deficient NP717 strain. We found that concomitant genetic deletion of *lipl-5* had no additive effect on the enhanced lifespan and reduced fat catabolism phenotypes exhibited by coelomocyte-deficient animals subjected to bacterial deprivation (Figures 6A and 6B; Table S2), suggesting that *lipl-5* and coelomocytes act via a similar and/or overlapping mechanism in mediating these phenotypes. Similarly, overexpression of *lipl-5* in coelomocyte-deficient animals (driven by the endogenous *lipl-5* promoter) failed to influence fat catabolism or lifespan extension in response to

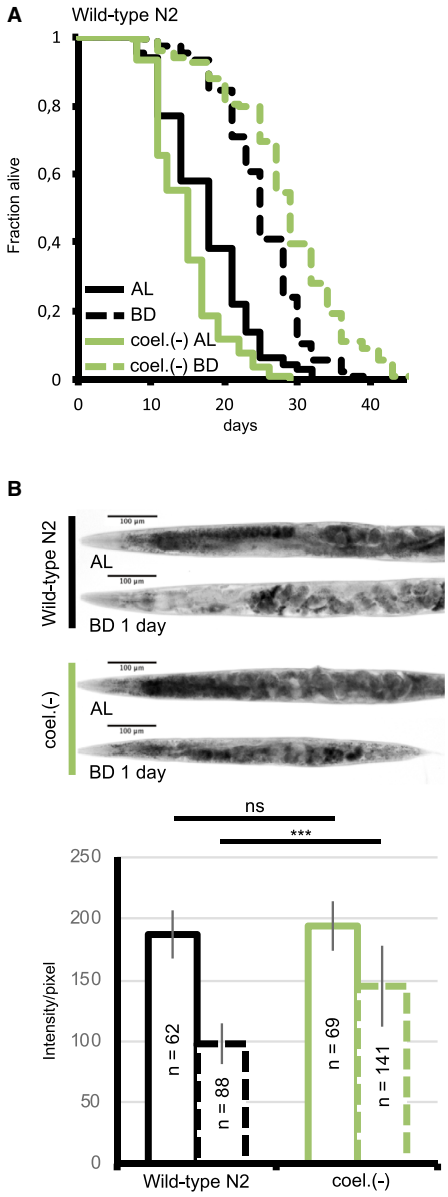

Figure 5. Coelomocyte-Deficient *C. elegans* Exhibit Decreased Fat Catabolism and Enhanced Lifespan Extension in Response to Bacterial Deprivation

(A) Lifespan analyses of *C. elegans* fed *ad libitum* (AL) or subjected to bacterial deprivation (BD). BD extended lifespan by 89% for coelomocyte-deprived animals ($p < 0.0001$) and by 42% for wild-type animals ($p < 0.0001$). In AL, the lifespan of coelomocyte-deprived animals was 16% shorter than that of wild-type animals ($p < 0.001$). In BD, the lifespan of coelomocyte-deprived animals was 12% longer than that of wild-type animals ($p < 0.001$). Mantel-Cox log-rank test. Representative of 6 replicate experiments (see Table S2 for number of replicates).

(B) Light micrographs of representative oil red O (ORO)-stained whole animals (upper panels) and densitometric quantification of staining of the two first intestinal cells after background removal (lower panels) of wild-type *C. elegans* and coelomocyte-deficient animals (coel.(−)) fed AL or subjected to BD for 1 day. Mean ± SD of n = at least 30 worms. ns, not significant; ***$p < 0.001$ by two-tailed Mann-Whitney U test. Representative of 6 biological replicates. See also Figure S6.

starvation (Figures 6C and 6D; Table S2). These data suggest that these functions of LIPL-5 are mediated predominantly in coelomocytes. To test this directly, we restored *lipl-5* expression only in the coelomocytes of *lipl-5(ok3581)* animals by using the coelomocyte-specific *unc-122* promoter. This was sufficient to reduce lifespan extension upon bacterial deprivation (Figure 7; Table S2). The ability to catabolize fat was also restored, although to a lesser extent. Intestinal TAG was lost more intensely upon bacterial deprivation, but this difference reached a statistical difference using one statistical test (two-tailed Student's t test), but not the other (two-tailed Mann-Whitney U test) (Figure 7A). These data suggest that the functions of coelomocytes in regulating fat catabolism and lifespan in response to bacterial deprivation are mostly mediated by LIPL-5. Our lifespan data do not exclude the involvement of other factors. Collectively, the results presented here uncover a role for coelomocytes in mediating both fat catabolism and lifespan phenotypes of *C. elegans* subjected to DR. The lipase LIPL-5 mediates both phenotypes, with the coelomocyte-localized enzyme playing a predominant role.

DISCUSSION

DR is a well-established longevity paradigm in numerous species, including humans (Redman et al., 2018). In this work, we tested the role of fat catabolism in regulating lifespan extension upon DR. We found that DR-induced lifespan extension in wild-type *C. elegans* is accompanied by a marked induction of LIPL-5 and a concomitant increase in catabolism of TAG stores. Animals subjected to *lipl-5* RNAi and *lipl-5(ok3581)* mutants showed diminished fat catabolism and extended longevity compared with wild-type animals upon bacterial deprivation. Thus, LIPL-5 may represent a nexus linking nutrient deprivation, fat catabolism, and longevity.

We found that LIPL-5 was mainly detectable in coelomocytes. Although this result was unexpected, we are confident that it was not an artifact induced by endocytosis of supra-physiological protein levels, because coelomocyte-specific staining was also observed when the endogenous *lipl-5* gene was replaced by a single copy of tagged LIPL-5 and expressed under the control of its own promoter. Whether LIPL-5 is produced within coelomocytes or is endocytosed from the pseudocoelom remains unclear. However, our data show that LIPL-5 can affect fat catabolism and lifespan when its expression is restricted to coelomocytes. These data therefore suggest that, independent of where *lipl-5* is expressed, its action mainly takes place in coelomocytes. We cannot firmly exclude that LIPL-5 may function marginally in other tissues as well. Animals lacking coelomocytes behaved similarly to *lipl-5* mutants under bacterial deprivation conditions, and concomitant loss of both coelomocytes and *lipl-5* did not have an additive effect on either fat catabolism or lifespan extension. However, coelomocyte-specific restoration of *lipl-5* expression in *lipl-5(ok3581)* mutants was sufficient to restore fat catabolism and longevity, although not quite fully. This result could imply a requirement for higher levels of LIPL-5 or expression in tissues other than coelomocytes to restore the wild-type longevity phenotype.

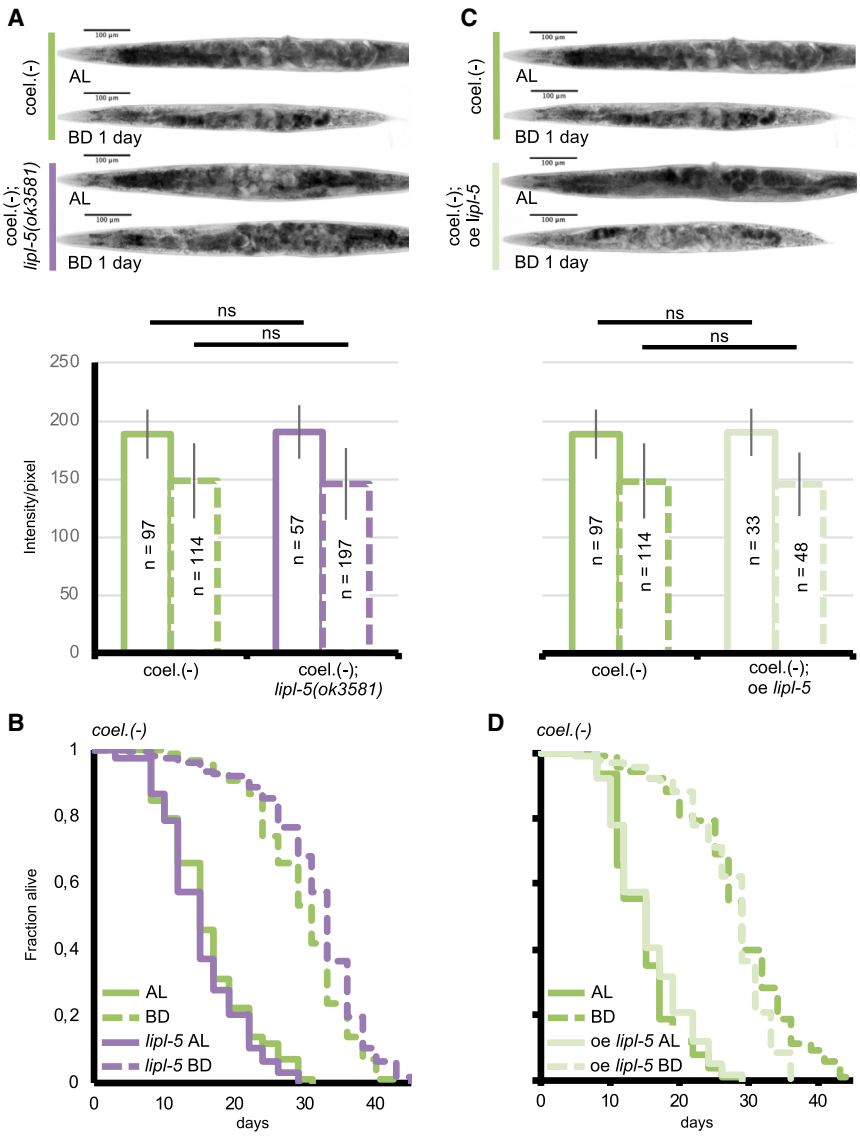

Figure 6. LIPL-5/LIPF Functions in Coelomocytes

(A and C) Light micrographs of representative oil red O (ORO)-stained whole animals (upper panels) and densitometric quantification of staining of the two first intestinal cells after background removal (lower panels) for coelomocyte-deficient single mutants (coel.(−)) (represented twice; A and C) and coel.(−);*lipl-5(ok3581)* double mutants (A) or coel.(−) mutants overexpressing *lipl-5* (C). Animals were fed *ad libitum* (AL) or subjected to bacterial deprivation (BD) for 1 day. Mean ± SD of n = 30. ns, not significant; *p < 0.05 by two-tailed Mann-Whitney U test. Representative of 3 biological replicates.

(B and D) Lifespan analyses of *C. elegans* fed AL or subjected to BD. (B) BD extended lifespan by 89% for coelomocyte-deprived animals ($p < 0.0001$) and by 106% for coelomocyte-deficient mutants for *lipl-5(ok3581)* ($p < 0.0001$). These two strains have similar lifespan in AL ($p = 0.185$), but coelomocyte-deprived mutants for *lipl-5(ok3581)* had lifespan increased by 12% in BD ($p < 0.05$) when compared with that of coelomocyte-deficient animals with a wild-type copy of *lipl-5*. (D) BD extended lifespan by 82% for coelomocyte-deficient animals ($p < 0.0001$) and by 93% for coelomocyte-deficient animals overexpressing *lipl-5* driven by its own promoter ($p < 0.0001$). These two strains have similar lifespan in AL ($p = 0.234$) and in BD ($p = 0.309$). Mantel-Cox log-rank test (see Table S2 for number of replicates).

In summary, we show here that coelomocytes can integrate nutrient-derived signals to influence both fat metabolism and lifespan in *C. elegans*. Our data thus provide another example of inter-tissue communication and support the notion that coelomocytes integrate nutritional signals (Fares and Greenwald, 2001). How coelomocytes communicate with the functions of other tissues, such as the intestine, remains unknown, and identifying new factors involved in this communication is an exciting prospect for future studies.

STAR★METHODS

Detailed methods are provided in the online version of this paper and include the following:

- KEY RESOURCES TABLE
- LEAD CONTACT AND MATERIALS AVAILABILITY
- EXPERIMENTAL MODEL AND SUBJECT DETAILS
  - Worm Strains
  - Strain Construction
- METHOD DETAILS
  - Plasmid Construction
  - Lifespan Assays
  - RT-qPCR
  - Oil Red O Staining of Neutral Lipids
  - Coelomocyte Imaging
  - Lipid Analysis by Thin Layer Chromatography
  - Sudan Black B Staining
- QUANTIFICATION AND STATISTICAL ANALYSIS
  - Statistical Analysis

SUPPLEMENTAL INFORMATION

Supplemental Information can be found online at https://doi.org/10.1016/j.celrep.2019.06.064.

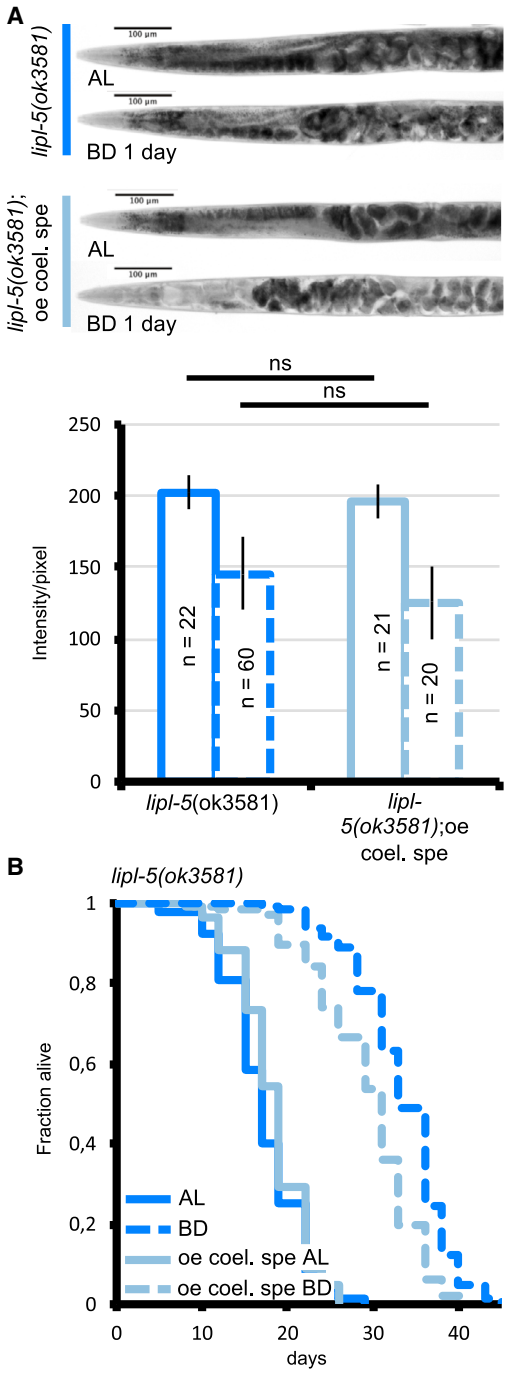

Figure 7. Coelomocyte-Localized LIPL-5/LIPF Rescues Bacterial Deprivation-Induced Fat Catabolism and Lifespan Extension in *lipl-5(ok3581)* Mutants

(A) Light micrographs of representative oil red O (ORO)-stained whole animals (upper panels) and densitometric quantification of staining of the two first intestinal cells after background removal (lower panels) for *lipl-5(ok3581)* mutants with or without coelomocyte-specific (*cc1*-driven) overexpression of *lipl-5*. Animals were fed *ad libitum* (AL) or subjected to bacterial deprivation (BD) for 1 day. Mean ± SD of n = at least 20 worms. ns, not significant; two-tailed Mann-Whitney U test. Representative of 3 biological replicates.

(B) Lifespan analyses of *C. elegans* fed AL or subjected to BD. BD extended lifespan by 83% for *lipl-5(ok3581)* mutants ($p < 0.0001$) and by 70% for *lipl-5(ok3581)* mutants overexpressing *lipl-5* specifically in coelomocytes ($p < 0.0001$). These two strains exhibit similar lifespan in AL ($p = 0.143$), but in BD, *lipl-5(ok3581)* mutant animals had a lifespan 12% longer when compared with *lipl-5(ok3581)* mutants overexpressing *lipl-5* specifically in coelomocytes ($p < 0.001$). Mantel-Cox log-rank test (see Table S2 for number of replicates).

ACKNOWLEDGMENTS

We thank all members of the Aguilaniu lab for fruitful discussions; the Caenorhabditis Genetics Center, which is funded by NIH Office of Research Infrastructure Programs (P40 OD010440); Marie Delattre, Johnny Fares, and Cynthia Kenyon for providing strains and reagents; and Anne O'Rourke for helpful comments on the manuscript. We also thank the PLATIM (Plateau Technique Imagerie/Microscopie IFR 128). This work was supported by an European Research Council grant to H.A. (H2020/2014-2019-N°647003).

AUTHOR CONTRIBUTIONS

A.B., J.G., and S.B. performed the experiments; L.M. helped with the staining and lifespan experiments; N.L. and H.G. performed the thin-layer chromatography (TLC) experiments; and H.A. conceived the study and wrote the paper.

DECLARATION OF INTERESTS

The authors declare no competing interests.

Received: May 24, 2018
Revised: February 24, 2019
Accepted: June 17, 2019
Published: July 23, 2019

REFERENCES

Afzal, S., Tybjærg-Hansen, A., Jensen, G.B., and Nordestgaard, B.G. (2016). Change in Body Mass Index Associated With Lowest Mortality in Denmark, 1976–2013. JAMA *315*, 1989–1996.

Bustos, V., and Partridge, L. (2017). Good Ol' Fat: Links between Lipid Signaling and Longevity. Trends Biochem. Sci. *42*, 812–823.

Fares, H., and Greenwald, I. (2001). Genetic analysis of endocytosis in *Caenorhabditis elegans*: coelomocyte uptake defective mutants. Genetics *159*, 133–145.

Gonzalez-Covarrubias, V. (2013). Lipidomics in longevity and healthy aging. Biogerontology *14*, 663–672.

Goudeau, J., Bellemin, S., Toselli-Mollereau, E., Shamalnasab, M., Chen, Y., and Aguilaniu, H. (2011). Fatty acid desaturation links germ cell loss to longevity through NHR-80/HNF4 in *C. elegans*. PLoS Biol. *9*, e1000599.

Greer, E.L., and Brunet, A. (2009). Different dietary restriction regimens extend lifespan by both independent and overlapping genetic pathways in *C. elegans*. Aging Cell *8*, 113–127.

Hansen, M., Flatt, T., and Aguilaniu, H. (2013). Reproduction, fat metabolism, and life span: what is the connection? Cell Metab. *17*, 10–19.

Kaeberlein, T.L., Smith, E.D., Tsuchiya, M., Welton, K.L., Thomas, J.H., Fields, S., Kennedy, B.K., and Kaeberlein, M. (2006). Lifespan extension in *Caenorhabditis elegans* by complete removal of food. Aging Cell *5*, 487–494.

Lapierre, L.R., Gelino, S., Meléndez, A., and Hansen, M. (2011). Autophagy and lipid metabolism coordinately modulate life span in germline-less *C. elegans*. Curr. Biol. *21*, 1507–1514.

Lapierre, L.R., Silvestrini, M.J., Nuñez, L., Ames, K., Wong, S., Le, T.T., Hansen, M., and Meléndez, A. (2013). Autophagy genes are required for normal lipid levels in *C. elegans*. Autophagy *9*, 278–286.

Masoro, E.J., Yu, B.P., and Bertrand, H.A. (1982). Action of food restriction in delaying the aging process. Proc. Natl. Acad. Sci. USA *79*, 4239–4241.

McKay, R.M., McKay, J.P., Avery, L., and Graff, J.M. (2003). *C. elegans*: a model for exploring the genetics of fat storage. Dev. Cell *4*, 131–142.

Narbonne, P., and Roy, R. (2009). *Caenorhabditis elegans* dauers need LKB1/AMPK to ration lipid reserves and ensure long-term survival. Nature *457*, 210–214.

Noble, T., Stieglitz, J., and Srinivasan, S. (2013). An integrated serotonin and octopamine neuronal circuit directs the release of an endocrine signal to control *C. elegans* body fat. Cell Metab. *18*, 672–684.

O'Rourke, E.J., and Ruvkun, G. (2013). MXL-3 and HLH-30 transcriptionally link lipolysis and autophagy to nutrient availability. Nat. Cell Biol. *15*, 668–676.

O'Rourke, E.J., Soukas, A.A., Carr, C.E., and Ruvkun, G. (2009). *C. elegans* major fats are stored in vesicles distinct from lysosome-related organelles. Cell Metab. *10*, 430–435.

O'Rourke, E.J., Kuballa, P., Xavier, R., and Ruvkun, G. (2013). ω-6 Polyunsaturated fatty acids extend life span through the activation of autophagy. Genes Dev. *27*, 429–440.

Park, J.-K., and Park, S.-K. (2017). Coelomocytes are required for lifespan extension via different methods of dietary restriction in *C. elegans*. Toxicol. Environ. Health Sci. *9*, 59–63.

Park, J.-K., Hwang, J.-K., Song, K.-H., and Park, S.-K. (2015). Role of Coelomocytes in Stress Response and Fertility in *Caenorhabditis elegans*. J. Life Sci. *25*, 263–268.

Redman, L.M., Smith, S.R., Burton, J.H., Martin, C.K., Il'yasova, D., and Ravussin, E. (2018). Metabolic Slowing and Reduced Oxidative Damage with Sustained Caloric Restriction Support the Rate of Living and Oxidative Damage Theories of Aging. Cell Metab. *27*, 805–815.e4.

Schroeder, E.A., and Brunet, A. (2015). Lipid Profiles and Signals for Long Life. Trends Endocrinol. Metab. *26*, 589–592.

Sutphin, G.L., and Kaeberlein, M. (2008). Dietary restriction by bacterial deprivation increases life span in wild-derived nematodes. Exp. Gerontol. *43*, 130–135.

Zhang, Y., Grant, B., and Hirsh, D. (2001). RME-8, a conserved J-domain protein, is required for endocytosis in *Caenorhabditis elegans*. Mol. Biol. Cell *12*, 2011–2021.

Zhang, S.O., Box, A.C., Xu, N., Le Men, J., Yu, J., Guo, F., Trimble, R., and Mak, H.Y. (2010). Genetic and dietary regulation of lipid droplet expansion in *Caenorhabditis elegans*. Proc. Natl. Acad. Sci. USA *107*, 4640–4645.

STAR★METHODS

KEY RESOURCES TABLE

REAGENT or RESOURCE	SOURCE	IDENTIFIER
Bacterial and Virus Strains		
Escherichia coli HT115	Ahringer library *Nature* 408, 325–330 (2000)	N/A
Escherichia coli RNAi lipl-1	Ahringer library *Nature* 408, 325–330 (2000)	N/A
Escherichia coli RNAi lipl-2	Ahringer library *Nature* 408, 325–330 (2000)	N/A
Escherichia coli RNAi lipl-3	Ahringer library *Nature* 408, 325–330 (2000)	N/A
Escherichia coli RNAi lipl-4	Ahringer library *Nature* 408, 325–330 (2000)	N/A
Escherichia coli RNAi lipl-5	Ahringer library *Nature* 408, 325–330 (2000)	N/A
Chemicals, Peptides, and Recombinant Proteins		
TRI Reagent ®	Sigma-Aldrich	T9424-100ML
2X MRWB (2% formaldehyde [methanol free], 160 mM KCl; 40 mM NaCl, 4 mM EGTA, 1 mM spermidine, 0.4 mM spermine, 30 mM PIPES, pH 7.4, and 0.2% β-mercaptoethanol)	O'Rourke et al., 2009	N/A
Critical Commercial Assays		
Gibson Assembly Kit	NEB	E5510S
RNeasy Mini Kits	QIAGEN	74104
iScript cDNA Synthesis kit	Bio-Rad	1708890
Experimental Models: Organisms/Strains		
N2 Bristol	CGC	N2
glp-1(e2141ts)III	Gift from Kenyon Lab	CF1903
daf-2(e1370)III	CGC	CB1370
lipl-5(ok3581)V	CGC	RB2573
lynEx03 = [(pAB02(lipl-5p::lipl-5::td-tomato) and co-injection marker myo-2p::mCherry]	UMS3421	MCP39
lipl-5(ok3581)V;lynEx03	Our lab	HGA2912
unc-119(ed3)III;pwIs50	CGC	RT258
pwIs50 = [lmp-1::GFP + Cbr-unc-119(+)]		
lipl-5::td-tomato	UMS3421	MCP34
lipl-5::td-tomato;pwIs50	Our lab	HGA2914
coel.(-)	Gift from Fares Lab	NP717
coel.(-);lipl-5(ok3581)V	Our lab	HGA2915
coel.(-);lynEx03	Our lab	HGA2916
lipl-5(ok3581)V;lynEx04	Our lab	HGA2917
lynEx04 = [(pAB02(pcc1::lipl-5::td-tomato) and co-injection marker myo-2p::mCherry]		
lipl-5(bab-8)V	UMS3421	MCP12
lipl-5(ok3581)V;lynEx02	Our lab	HGA8021
lynEx02 = [(pAB01(ges-1p::lipl-5::gfp) and co-injection marker myo-2p::mCherry]		
Oligonucleotides		
See Table S3 for oligonucleotide information		N/A

(*Continued on next page*)

Continued

REAGENT or RESOURCE	SOURCE	IDENTIFIER
Recombinant DNA		
pHD43 plasmid	kindly provided by Hanna Fares, University of Arizona Cancer Center	N/A
pPD95.75-Pges-1 plasmid	kindly provided by Hideki Inoue, Pittsburgh University	N/A
pCFJ90: *myo-2p::mCherry*	Addgene	http://www.addgene.org/19327/
Software and Algorithms		
ImageJ		https://imagej.nih.gov/ij/
two-tailed Mann-Whitney U test	This paper	https://www.socscistatistics.com/tests/mannwhitney/default2.aspx
two-tailed Student's t test	This paper	https://www.xlstat.com/fr/
Mantel–Cox log-rank	This paper	https://www.xlstat.com/fr/
WinCATS software	This paper	https://www.camag.com/en/tlc_hptlc/support services/software/wincats_releases.cfm?command=archive

LEAD CONTACT AND MATERIALS AVAILABILITY

Further information and requests for resources and reagents should be directed to and will be fulfilled by the Lead Contact, Hugo Aguilaniu (haguilaniu@gmail.com).

EXPERIMENTAL MODEL AND SUBJECT DETAILS

Worm Strains

Nematodes were grown and maintained under standard conditions. N2 Bristol was used as the wild-type strain. All other strains and their origins are listed in Table S1.

Strain Construction

Double mutant strains were generated using standard genetic procedures. *lipl-5 (ok3581)* mutants were backcrossed five times, and the presence of the *lipl-5(ok3581)* mutation was confirmed by PCR using allele-specific primers. We confirmed that the NP717 strain lacked coelomocytes by testing for the coelomocyte uptake (cup) phenotype where GFP is taken up within the pseudoceolom. To generate transgenic animals, pAB01(*ges-1p::lipl-5::gfp*) was injected at 50 ng/μL, pAB02(*lipl-5p::lipl-5::tdTOMATO*) and pAB03 (*pcc1::lipl-5::tdTOMATO*) were injected at 10 ng/μL, as previously described (ref?), and the *myo-2p::mCherry* (pCFJ90) marker was co-injected at 2.5 ng/μL. These transgenes were named lynEx02, lynEx03, and lynEx04, respectively. The *myo-2p::mCherry* marker and empty vectors used here were confirmed to have no effect on lifespan (data not shown). CRISPR insertions for *lipl-5(bab-8)* and *lipl-5::tdTOMATO* were generated by the UMS3421. The *lipl-5(bab-8)* mutant was created by inserting an ED10-Hygro-HisClo cassette into the *lipl-5* locus and then removing it to leave a 20 bp scar in place of the *lipl-5* gene. The *lipl-5::tdTOMATO* strain was generated by insertion of a tdTOMATO-tagged version of LIPL-5 instead of the cassette.

METHOD DETAILS

Plasmid Construction

The plasmid pAB01(*ges-1p::lipl-5::gfp*), encoding GFP-tagged LIPL-5 driven by the intestine-specific *ges-1* promoter, was constructed by amplifying the *lipl-5* open reading frame (ORF) from genomic DNA (from the start codon to the end of *lipl-5* gene before the stop codon) using SalI and KpnI primers (SalI/lipl-5 F: 5′-CTGGTCGACATGTGGC GGTTTGCCGTTTTTC-3′; lipl-5/KpnI R: 5′-GTGGTACCTTTCCCAAATAATCGTCAG TGCACAGC-3′). The fragment was inserted into the worm expression vector pPD95.75-Pges-1 (kindly provided by Hideki Inoue, Pittsburgh University) upstream and in-frame with the GFP sequence and downstream and in-frame with the *ges-1* promoter. Essential parts of the final plasmid pAB01 were sequenced to verify that the *lipl-5* sequence was in-frame with the *ges-1* promoter and GFP sequences.

The plasmid pAB02 (*lipl-5p::lipl-5::tdTOMATO*), encoding tdTOMATO-tagged LIPL-5 driven by the endogenous promoter, was constructed by amplifying a fragment starting 1.5 kb upstream of and extending through the *lipl-5* ORF, excluding the last stop codon, from genomic DNA using a Gibson Assembly Kit (primers: lipl-5p/lipl-5 gibson F: 5′-CAC AAC GAT GGA TAC GCT AAC AAC TTG GAA ATG AAA TAA GCT TCT AAA ACA ATT ATT TTC AGA CGA TAC TTG GTC-3′; lipl-5p/lipl-5 gibson R: 5′-GAT GAC

CTC CTC GCC CTT GCT CAC CAT TAC CGG TAC CGA TTT TCC CAA ATA ATC GTC AGT GC-3′). The fragment was inserted into the worm expression vector sur-5::td-tomato (kindly provided by Dr. Ehud Cohen, Hebrew University) upstream and in-frame with the td-tomato sequence. Essential parts of the final plasmid pAB02 were sequenced to confirm that the *lipl-5* promoter and gene sequences were in-frame with td-tomato.

The plasmid pAB03 (*pcc1::lipl-5::tdTOMATO*), encoding tdTOMATO-tagged LIPL-5 driven by the coelomocyte-specific promoter *pcc-1*, was constructed by amplifying a 180 bp sequence upstream of *unc-122* from the pHD43 plasmid (kindly provided by Hanna Fares, University of Arizona Cancer Center), which was previously described as the coelomocyte promoter (Fares and Greenwald, 2001), and the *lipl-5* gene, excluding the last stop codon, from genomic DNA. The two fragments were inserted into the pAB02 plasmid to replace the *lipl-5* promoter and gene, upstream and in-frame with the td-tomato sequence, using a Gibson Assembly Kit (primers PCR1 F1 (Plasmid+Pcc1): 5′-CGC TAA CAA CTT GGA AAT GAA ATA AGC TTG TTG ACA CGC AGT TTC CCT-3′; PCR1 R1F2 (Pcc1+lipl-5): 5′-AAC GGC AAA CCG CCA CAT ATT GTG AGC CCA ATG AAG TAA AAT TTC-3′; PCR2 R1F2 (Pcc1+lipl-5): 5′-GAA ATT TTA CTT CAT TGG GCT CAC AAT ATG TGG CGG TTT GCC GTT-3′; PCR2 R2 (lipl-5+Plasmid): 5′-CCC TTG CTC ACC ATT ACC GGT ACC GAT TTT CCC AAA TAA TCG TCA GTG CAC-3′). Essential parts of the final plasmid pAB03 were sequenced to confirm that the coelomocyte promoter sequence was in-frame with the *lipl-5* gene and td-tomato.

Lifespan Assays

Lifespan assays were conducted according to standard protocols (Goudeau et al., 2011) at 20°C, starting from day 1 of adulthood. Our assay was performed at 20°C. Lifespan assays were conducted on plates supplemented with 15 μM 5-fluorouracil to prevent progeny from hatching. For BD experiments, plates contained 50 μM kanamycin, which was confirmed to not affect lifespan (unpublished data), and worms were washed 3 times in M9 buffer prior to experiments. Contaminated worms, or those crawling off the plate, exploding, or bagging were censored at the time of their loss.

RT-qPCR

Primer sequences are provided in the STAR Methods. In brief, synchronized L1 larvae were grown at 25°C on ht115 *E. coli* until they reached day 1 of adulthood. For RNAi experiments, worms were grown on ht115 *E. coli* bacteria carrying empty vector or expressing dsRNA against the gene of interest. The BD experiments, worms were transferred to bacteria-free plates and suppression of target gene expression was verified at the end of the experiment. Animals were collected, washed, and frozen at −80°C for at least 24 h before RNA was extracted using TRI Reagent ® (MRC Molecular Research Center) and RNeasy Mini Kits (QIAGEN). The concentration and purity of RNA samples were determined using a DropSense (Trinean) spectrophotometer. cDNA was synthesized from aliquots of 1 μg of RNA using an iScript cDNA Synthesis kit (Bio-Rad). Quantitative PCR was performed using the StepOnePlus System (Applied Biosystems) according to the manufacturer's recommended protocol. Relative mRNA levels were normalized to the housekeeping genes *pmp-3, act-1,* and *cdc-42*. Primers are listed in the Supplemental Information.

Primers were designed with Primer 3. PMP-3 F: 5′-GTT CCC GTG TTC ATC ACT CAT-3′ and R: 5′-ACA CCG TCC AGA AGC TGT AGA-3′; CDC-42 F: 5′-CTG CTG GAC AGG AAG ATT ACG-3′ and R: 5′-CTC GGA CAT TCT CGA ATG AAG-3′; ACT-1 F: 5′-GCT GGA CGT GAT CTT ACT GAT TAC C-3′ and ACT-1 R: 5′-GTA GCA GAG CTT CTC CTT GAT GTC-3′; LILP-1 F: 5′-CGG TTT GCG CTG GAC TTA-3′ and R: 5′-GAA CAC GAG TTG CGT TAA-3′; LIPL-2 F: 5′-TGG ATG CAG ATG GTT CGC AA-3′ and R: 5′-GCC CTT GAT GGC TCC GAA AT-3′; LIPL-3 F: 5′-GCT CGT GAT TCT TGC GGT TC-3′ and R: 5′-CGG ATA ACC CCA TCG CTC AA-3′; LIPL-4 F: 5′-GAA ACG TTG TTC GCG CAG TT-3′ and R: 5′-AAC TTG GCT GGC TGC ATT TG-3′; LIPL-5 F: 5′-ACT GGG GAA CCA AGA CGA AC-3′ and R: 5′-TAT CAG CCA ACC AAT CGG CA-3′.

Oil Red O Staining of Neutral Lipids

Approximately 200 worms per sample were collected in phosphate-buffered saline (PBS) without $MgCl_2$ and resuspended in a buffer composed of 120 μL of PBS 1X and 120 μL of 2X MRWB (2% formaldehyde [methanol free], 160 mM KCl; 40 mM NaCl, 4 mM EGTA, 1 mM spermidine, 0.4 mM spermine, 30 mM PIPES, pH 7.4, and 0.2% β-mercaptoethanol). Samples were shaken for 1 h at 20°C, washed twice with PBS, incubated in 1 mL 60% isopropanol for 15 min at 20°C, and transferred to 1mL 60% Oil Red O solution overnight. After two washes with PBS, worms were resuspended in 200 μL PBS containing 0.001% Triton X-100, mounted between a slide and coverslip, and observed on a Nikon Eclipse 80i microscope with a 10 × objective. Images were captured with a monochrome digital camera (DS-Qi1Mc). Densitometric quantification of staining (expressed as intensity/pixel) was performed with ImageJ software on the two first intestinal cells after background removal. All experiments analyzed at least 20 worms per condition per point.

Coelomocyte Imaging

Worms were grown and maintained under standard conditions. Images of at least 25 worms were captured at 100 × , 400 × , and 1000 × magnification using 800 ms, 400 ms, and 800 ms exposure times, respectively. At least 4 of the 6 coelomocytes present in each worm were imaged. Worms were imaged on a Nikon Eclipse 80i microscope equipped with a monochrome digital camera (DS-Qi1Mc), and artificial color was added with ImageJ.

Lipid Analysis by Thin Layer Chromatography

Each sample consisted of a worm extract equivalent to 25μg soluble protein adjusted to 2 mL with distilled water. Cholesterol (2 μg) was added to each sample as an internal standard. Samples were mixed with 100 μL acetic acid, 2.3 mL methanol, and 2.3 mL chloroform and incubated for 5 min. The upper phase was discarded, and the organic phase was washed twice with 1 mL water/methanol/chloroform (2/2.5/2.5 v/v), dried under nitrogen, dissolved in 50 μL chloroform/methanol (1/1), and analyzed. A 10 μL aliquot of each sample was spotted onto 20 × 10 cm HPTLC Silicagel 60 plates (Merck, Germany) alongside six dilutions of a standard solution (50 ng/μL squalene, cholesterol palmitate, triolein, 1,3-diolein, 1,2-diolein, cholesterol, 25-hydroxy cholesterol, monoolein, and 1,2-dipalmitoyl-phosphocholine), and subjected to a multistep development procedure: (i) chloroform/ diethyl ether/ethyl acetate/methanol/acetic acid (76/6/20/2:1) to 4.5 cm from the lower edge of the plate, (ii) n-hexane/diethyl ether/acetic acid (80/20/1) to 6 cm, and (iii) n-hexane/acetic acid (100/1) to 80 cm. Plates were dried for 5 min after each development step. Bands were detected by immersion in a charring solution and drying at 250°C for 1 min and quantified densitometrically using a CAMAG TLC Scanner 4 and WinCATS software in absorption mode at 560 nm using a tungsten lamp. Samples were quantified by comparison with the standard curve spotted on each plate. Each analysis was performed in triplicate.

Sudan Black B Staining

Sudan Black B staining of lipids was performed on animals fed *ad libitum* (AL) or starved (BD) for 48 h. Worms were grown at 25°C from the L1 to the L4 stage and then shifted at 20°C. About 400 worms per sample were washed 4 times in M9 buffer and once with PBS + 20% Tween. The supernatant was removed, and 200 μL of PBS was added to the BD samples and 200 μL PBS plus 20 μL of 0.5 mg/mL 4′,6-diamidino-2-phenylindole (DAPI) was added to the AL samples. Fresh 1% paraformaldehyde in PBS was added to the worm pellet and incubated for 30 min at room temperature with stirring. Worms were then subjected to three cycles of freeze-thawing in liquid nitrogen and a 37°C water bath, incubated for 10 min on ice, and washed with M9. AL and BD worms were pooled, washed sequentially with 25%, 50%, and 70% ethanol, and then incubated overnight in Sudan Black B solution (50% saturated solution; 15 mg/mL in 70% ethanol). Animals were washed again in 70%, 50%, and 25% ethanol, resuspended in glycerol, and mounted animals on slides. Worms were imaged and photographed using a Nikon Eclipse 80i (Zeiss) microscope equipped with a monochrome digital camera (DS-Qi1Mc).

QUANTIFICATION AND STATISTICAL ANALYSIS

Statistical Analysis

Results are expressed as the mean ± standard deviation (SD) of triplicates, and all experiments were performed at least three times. For ORO experiments, value of n can be found in figure. Group differences were analyzed using a two-tailed Student's t test (parametric) or a two-tailed Mann-Whitney U test (non-parametric). Tests used are indicated in the figure legend. For lifespan assays, Excel XLStat was used to calculate the mean and maximal lifespans and differences were analyzed using the Mantel–Cox log-rank test. Value of n (number of worms) can be found in the Table S2. A p value of < 0.05 was considered statistically significant.

Cell Reports, Volume *28*

Supplemental Information

Coelomocytes Regulate Starvation-Induced Fat Catabolism and Lifespan Extension through the Lipase LIPL-5 in *Caenorhabditis elegans*

Alexia Buis, Stéphanie Bellemin, Jérôme Goudeau, Léa Monnier, Nicolas Loiseau, Hervé Guillou, and Hugo Aguilaniu

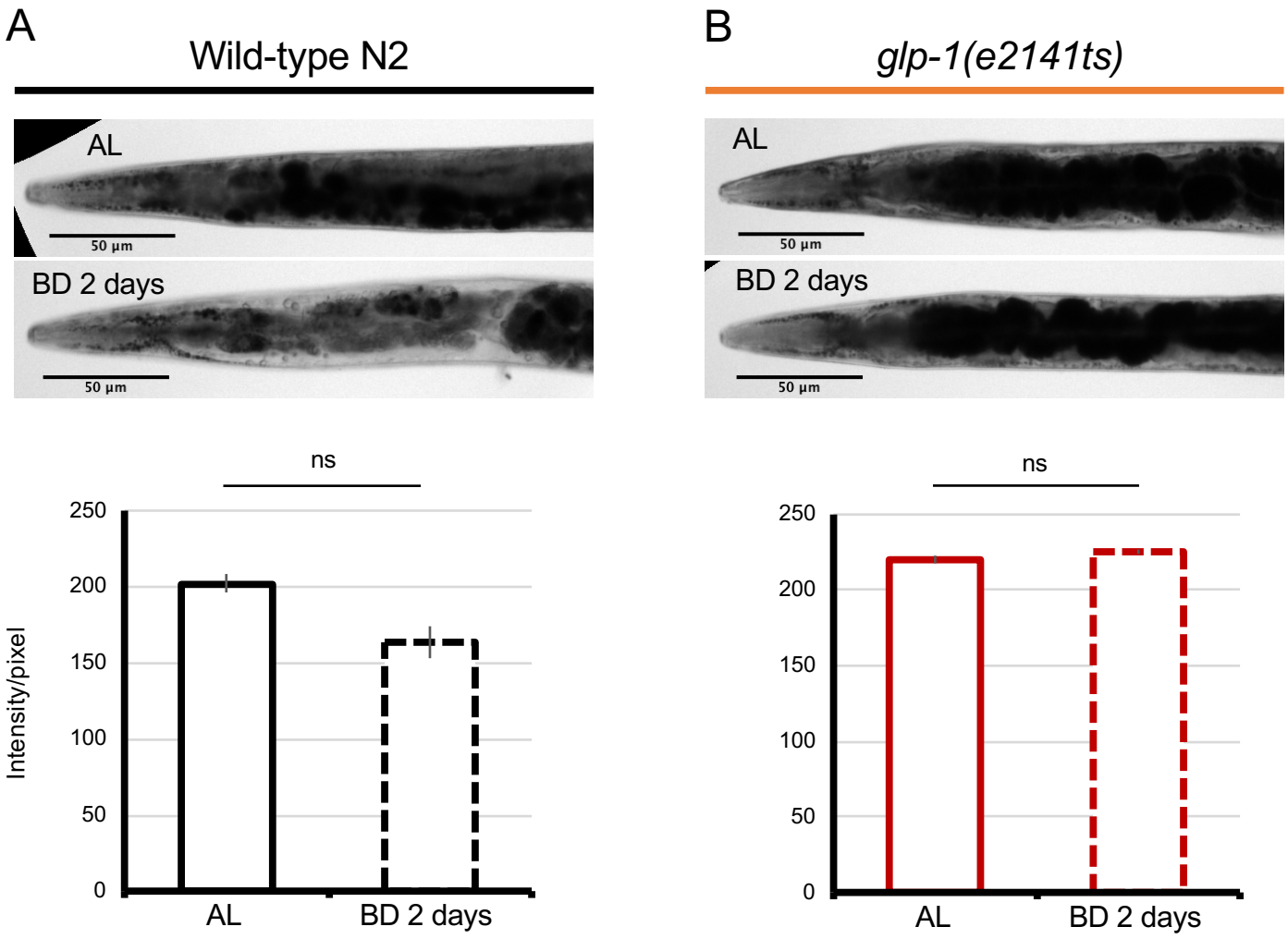

Figure S1. Sudan Black Staining of Lipids in Fed and Starved *C. elegans.*

Relates to Figure 1

(A and B) Sudan Black staining of representative whole animals (upper panels) and densitometric quantification of staining of the two first cells of the intestine after background removal (lower panels) in wild-type *C. elegans* and *glp-1(e2141ts)* mutants fed *ad libitum* (AL) or subjected to bacterial deprivation (BD) for 2 days. Mean ± SD of n 6. ns, not significant by two-tailed Mann-Whitney U test. Representative of 3 biological replicates.

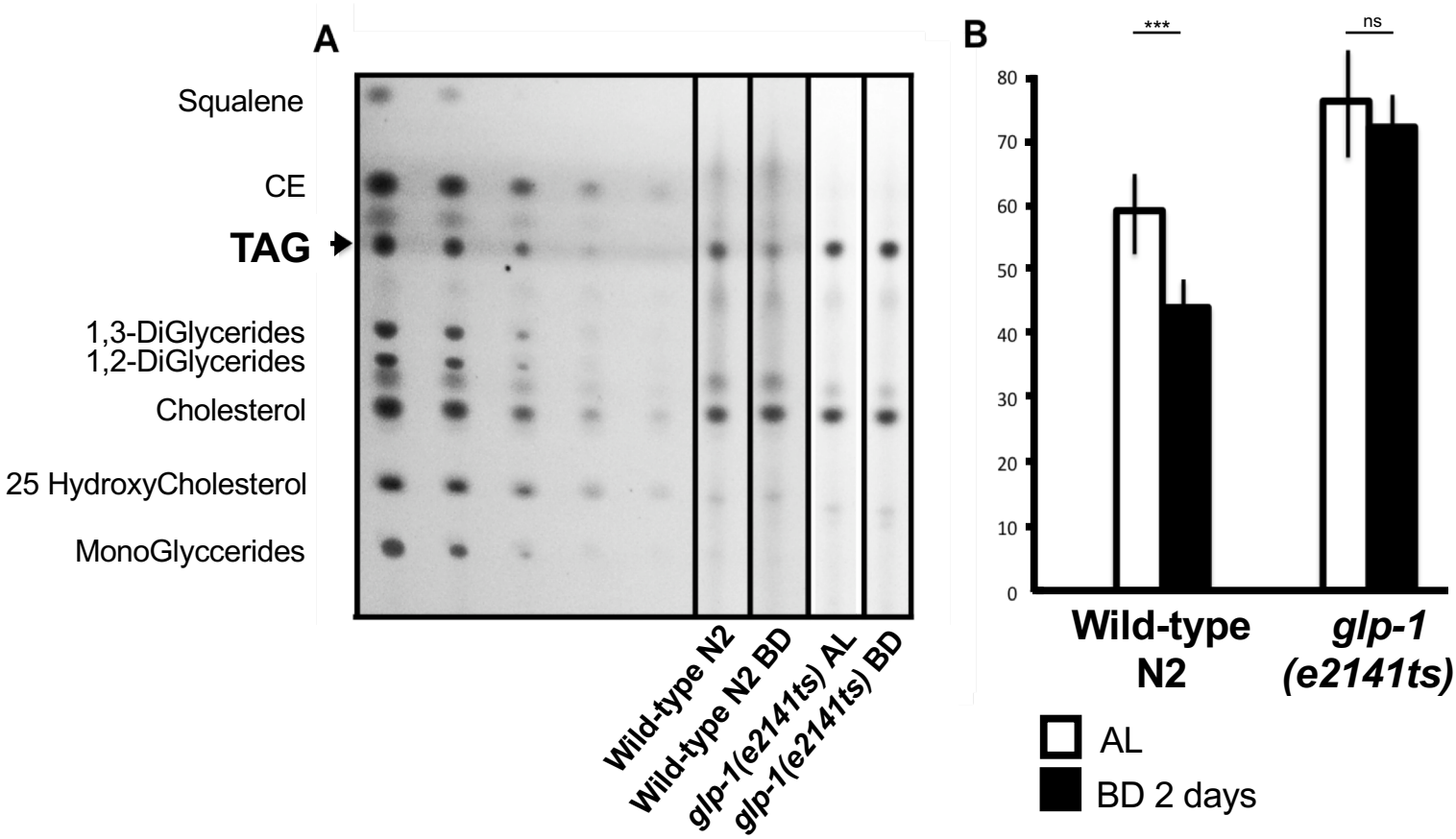

Figure S2. Thin Layer Chromatography of Lipids in Fed and Starved *C. elegans.*

Relates to Figure 1

(A) Thin layer chromatography of triacylglycerol (TAG) in wild-type N2 fed *ad libitum* (AL) or subjected to bacterial deprivation (BD) for 2 days. (B) Quantification of TG levels. Mean ± SD of n = at least 6. ns, not significant; *** $p < 0.001$ by two-tailed Student's t-test. Representative of 2 biological replicates.

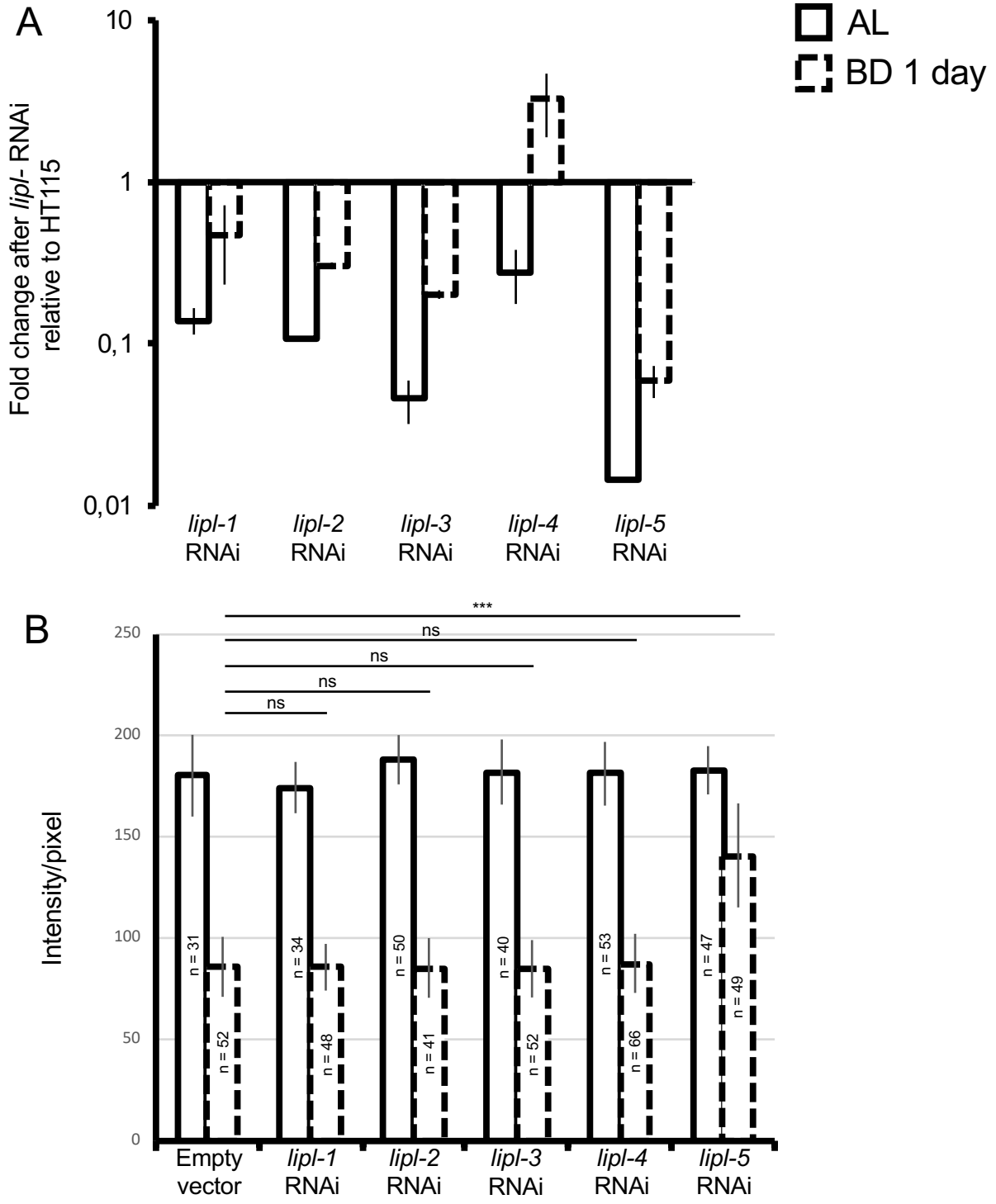

Figure S3. *lipl-1-5* RNAi Efficiency and Effect on Fat Catabolism in Fed and Starved *C. elegan*

Relates to Figure 1

(A) RT-qPCR analysis of *lipl-1*, *lipl-2*, *lipl-3*, *lipl-4*, and *lipl-5* mRNA in wild-type *C. elegans* subjected to RNAi and fed *ad libitum* (AL, solid bars) or subjected to bacterial deprivation (BD, dashed bars) for 1 day. Results are normalized to mRNA levels in animals fed bacteria transfected with empty vector. Representative of 3 biological replicates. The relatively inefficiency of *lipl-4* RNAi after 1 day of BD is likely due to the particularly strong induction of this lipase by BD. Note, however, that this isoform has little effect on TAG levels under these conditions (O'Rourke et al., 2013). (B) Densitometric quantification of Oil Red O staining of fat stores of the two first intestinal cells after background removal in wild-type *C. elegans* subjected to *lipl-1*, *-2*, *-3*, *-4*, or *-5* RNAi and fed AL (solid bars) or subjected to BD (dashed bars) for 1 day. Mean ± SD of n = at least 20 worms ns, not significant; ***$p < 0.001$ by two-tailed Mann-Whitney U test. Representative of 3 biological replicates.

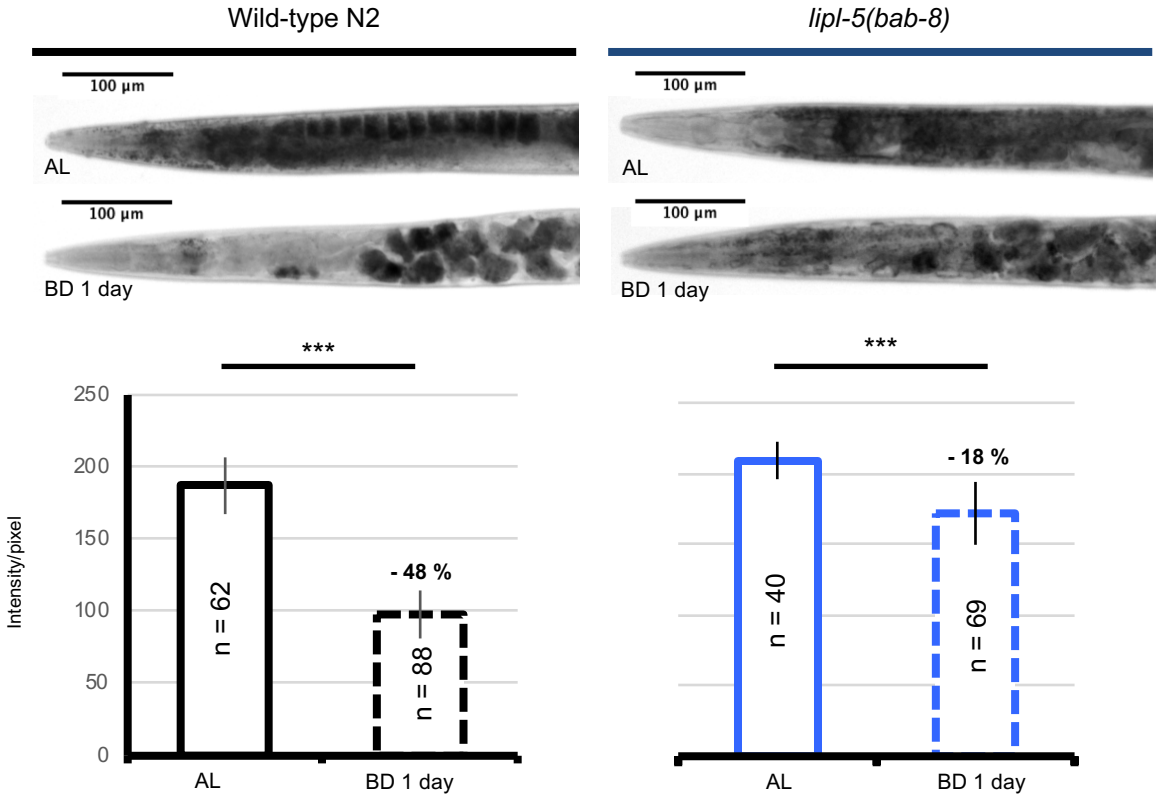

Figure S4. A Second *lipl-5* Mutation Confirms that Suppression of LIPL-5 Activity Mediates the Reduction in Fat Catabolism and Enhancement in Longevity Induced by Bacterial Deprivation
Relates to Figure 2

Light micrographs of representative Oil Red O (ORO)-stained whole animals (upper panels) and densitometric quantification of staining of the two first intestinal cells after background removal (lower panels) for wild-type *C. elegans* and *lipl-5(bab-8)* CRISPR-generate mutants fed *ad libitum* (AL) or subjected to bacterial deprivation (BD) for 1 day. Mean ± SD of n = 20. ***P < 0.001 by two-tailed Mann-Whitney U test. Representative of 5 biological replicates.

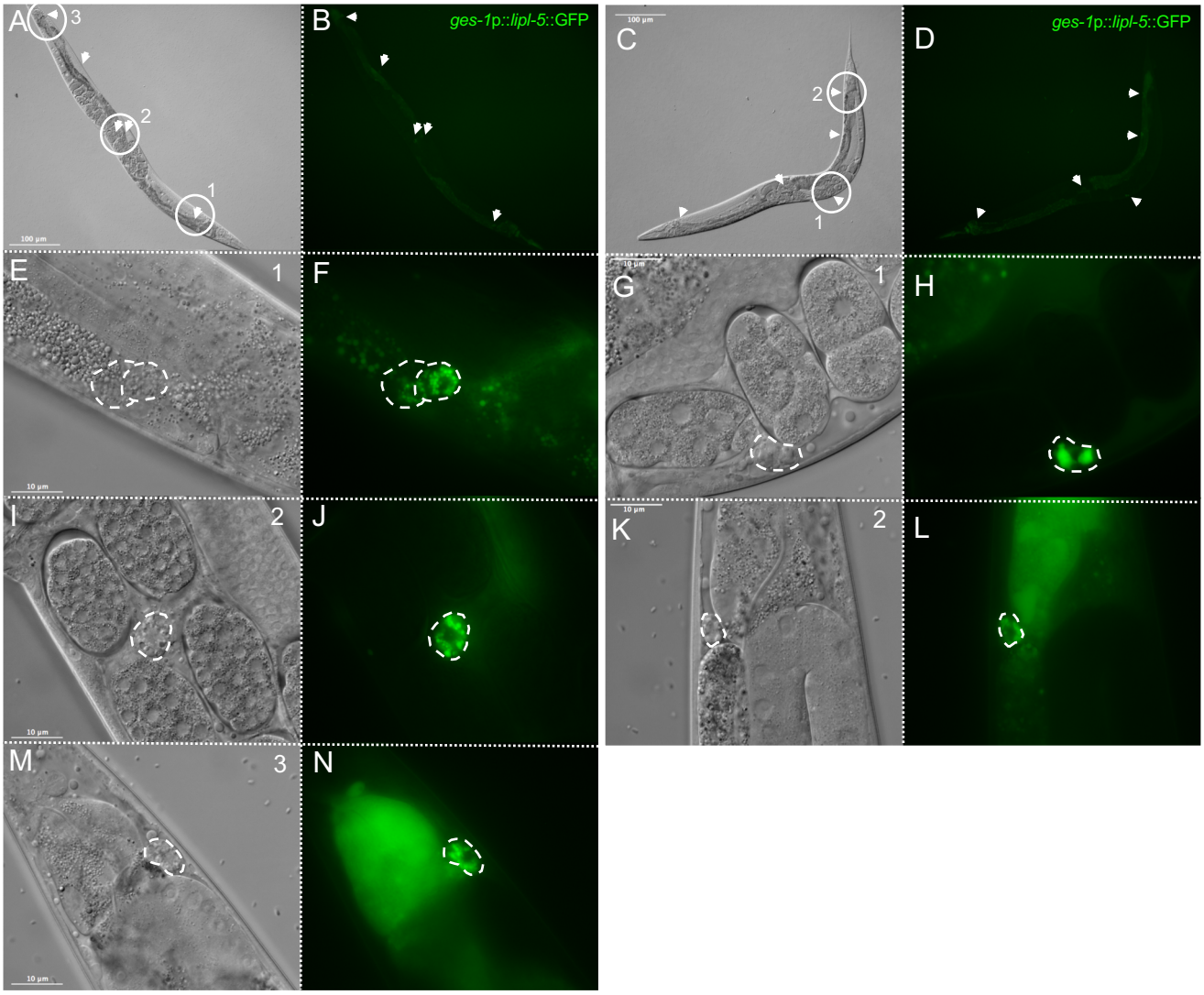
A
B
ges-1p::lipl-5::GFP
C
D
ges-1p::lipl-5::GFP
E
F
G
H
I
J
K
L
M
N
1
2
3

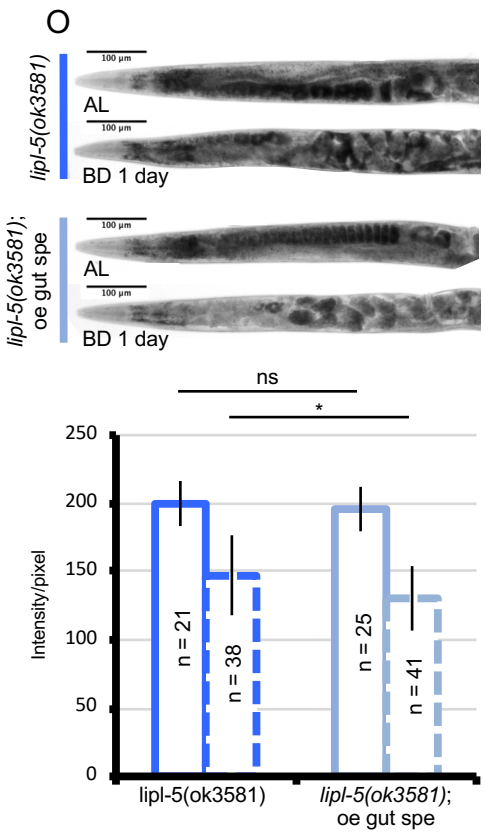
O
lipl-5(ok3581)
AL
BD 1 day
lipl-5(ok3581); oe gut spe
AL
BD 1 day
ns
*
Intensity/pixel
250
200
150
100
50
0
n = 21
n = 38
n = 25
n = 41
lipl-5(ok3581)
lipl-5(ok3581); oe gut spe

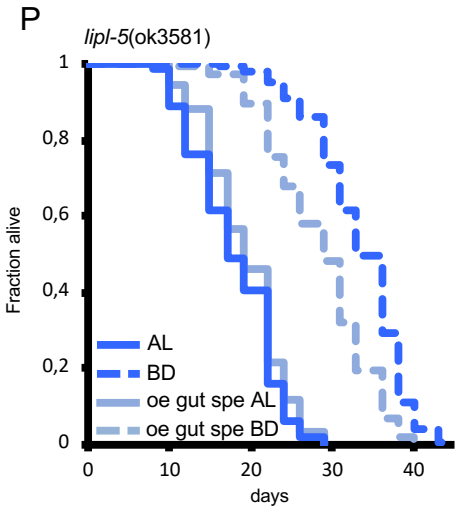
P
lipl-5(ok3581)
Fraction alive
1
0,8
0,6
0,4
0,2
0
AL
BD
oe gut spe AL
oe gut spe BD
0
10
20
30
40
days

Figure S5. Gut-specific lipl-5 Overexpression in lipl-5(ok358) Mutants Partially Reverses the Reduced Fat Catabolism and Enhanced Lifespan Extension Induced by Bacterial Deprivation.

Relates to Figure 2

(A, C, E, G, I, K, M) DIC images and (B, D, F, H, J, L, N) fluorescence images of *lipl-5(ok358)* mutants overexpressing LIPL-5::GFP in the gut (*ges-1* promoter). The A, C, E, G, I, K and M panels and right 6 panels show two adult animals at low magnification (A, B, C and D) and high magnification (E, F, G H, I, J, K, L, M, N); scale bars, 100 μm and 10 μm, respectively). White arrows and dotted lines indicate coelomocytes. Each experiment was replicated at least 3 times (biological replicates). (O) Light micrographs of representative Oil Red O (ORO)-stained whole animals (upper panels) and densitometric quantification of staining of the two first intestinal cells after background removal (lower panel) for *lipl-5(ok358)* mutants with or without gut specific (*ges-1*-driven) *lipl-5* overexpression. Animals were fed ad libitum (AL) or subjected to bacterial deprivation (BD) for 1 day. Mean ± SD of n = at least 20 worms ns, not significant; ** $p < 0.001$ by two-tailed Mann-Whitney U test. Representative of 3 biological replicates. (P) Lifespan analyses of *C. elegans* fed AL or subjected to BD. BD extended lifespan by 85% for *lipl-5(ok3581)* mutant ($P < 0.0001$) and by 48% for *lipl-5(ok3581)* mutants over-expressing lipl-5 specifically in the intestine ($P < 0.0001$). When fed ad libitum, the latter strain exhibits a 7% increase when compared to *lipl-5(ok3581)* mutant animals ($P < 0.05$). In BD, *lipl-5(ok3581)* mutants over-expressing lipl-5 specifically in the intestine live 14% shorter than simple *lipl-5(ok3581)* mutant animals ($P < 0.001$). Mantel-Cox log-rank test and the two-tailed Student's t-test. Representative of 3 replicate experiments (See table S2 for number of replicates).

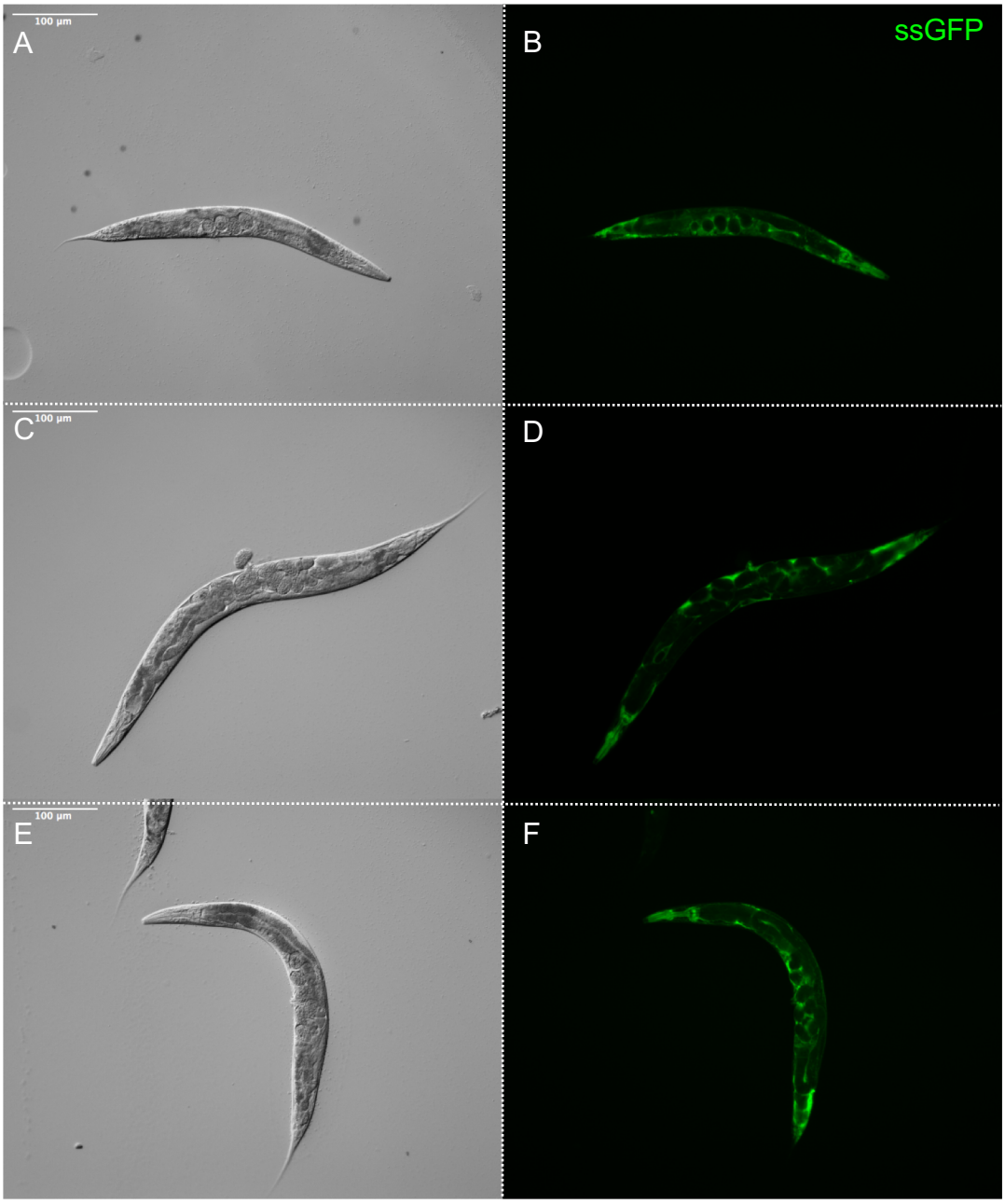

Figure S6. Coelomocyte-Deficient Animals Exhibit a Cup Phenotype.
Relates to Figure 5

(A, C, E) DIC images and (B, C, F) fluorescence images of adult coelomocyte-deficient animals (coel.(-)) expressing a soluble form of GFP secreted from body wall muscle cells. In wild-type *C. elegans*, GFP secreted into the pseudocoelom is taken up by coelomocytes; in coel.(-) animals, worms imaged, GFP accumulates in the pseudocoelom (coelomocyte uptake [cup] phenotype).

Genotype	Origin	Strain number
glp-1(e2141ts)III	Gift from Kenyon Lab	CF1903
daf-2(e1370)III	CGC	CB1370
lipl-5(ok3581)V	CGC	RB2573
lynEx03**	UMS3421	MCP39
lipl-5(ok3581)V;lynEx03	Our lab	HGA2912
unc-119(ed3)III;pwIs50***	CGC	RT258
lipl-5 ::td-tomato	UMS3421	MCP34
lipl-5 ::td-tomato;pwIs50	Our lab	HGA2914
coel.(-)	Gift from Fares Lab	NP717
coel.(-);*lipl-5(ok3581)V*	Our lab	HGA2915
coel.(-);lynEx03	Our lab	HGA2916
lipl-5(ok3581)V;lynEx04****	Our lab	HGA2917
lipl-5(bab-8)V	UMS3421	MCP12
lipl-5(ok3581)V;lynEx02******	Our lab	HGA8021

* CGC = Caenorhabditis Genetics Center
**lynEx03 = [(pAB02(*lipl-5p::lipl-5* ::td-tomato) and co-injection marker *myo-2p* ::mCherry]
***pwIs50 = [*lmp-1* ::GFP + *Cbr-unc-119* (+)]
****lynEx04 = [(pAB02(*pcc1::lipl-5:* ::td-tomato) and co-injection marker *myo-2p* ::mCherry]
*****bIs1 = [*vit-2* ::GFP + *rol-6(su1006)*]
******lynEx02 = [(pAB01(*ges-1p::lipl-5* ::gfp) and co-injection marker *myo-2p* ::mCherry]

Table S1: Strain list, Related to all figures

	Genotype	Condition	Mean LS	±	# Worms	% Change	P value
Figure 1 A	Wild-type N2	AL	16,372	0,411	194/201	62,98	< 0.0001
		BD	26,683	0,558	188/194		
	Wild-type N2	AL	17,703	0,621	132/139	31,78	< 0.0001
		BD	23,329	0,500	146/190		
	Wild-type N2	**AL**	**15,881**	**0,396**	**190/198**	**57,64**	**< 0.0001**
		BD	**25,035**	**0,446**	**144/176**		
Figure 4 A	**Wild-type N2**	**AL**	**18,495**	**0,318**	**233/239**	**56,42**	**< 0.0001**
		BD	**28,930**	**0,401**	**228/239**		
	Wild-type N2	AL	17,638	0,527	118/126	41,84	< 0.0001
		BD	25,017	0,569	95/116		
	Wild-type N2	AL	20,150	0,600	120/124	47,59	< 0.0001
		BD	29,740	0,640	100/129		
	lipl-5(ok3581)	AL	16,959	0,408	122/123	98,53	< 0.0001
		BD	33,668	0,396	131/142		
	lipl-5(ok3581)	**AL**	**18,162**	**0,474**	**122/124**	**85,57**	**< 0.0001**
		BD	**33,703**	**0,476**	**99/146**		
	lipl-5(ok3581)	AL	16,929	0,278	267/284	79,10	< 0.0001
		BD	30,320	0,398	157/171		
	Wild-type N2	AL	**18,495**	**0,318**	**233/239**	-1,80	0.515
	lipl-5(ok3581)		**18,162**	**0,474**	**122/124**		
	Wild-type N2	BD	**28,930**	**0,401**	**228/239**	16,50	P < 0.001
	lipl-5(ok3581)		**33,703**	**0,476**	**99/146**		
Figure 4 B	*lipl-5(ok3581)*	AL	18,653	0,492	98/103	85,20	< 0.0001
		BD	34,546	0,428	86/146		
	lipl-5(ok3581)	AL	18,653	0,492	98/103	85,20	< 0.0001
		BD	34,546	0,428	86/146		
	lipl-5(ok3581)	**AL**	**18,160**	**0,510**	**111/141**	**72,25**	**< 0.0001**
		BD	**31,280**	**0,770**	**67/109**		
	lipl-5(ok3581); oe *lipl-5 (endogenous promoter)*	AL	18,178	0,361	189/193	64,10	< 0.0001
		BD	29,830	0,455	126/144		
	lipl-5(ok3581);* oe *lipl-5 (endogenous promoter)	**AL**	**18,410**	**0,400**	**136/141**	**50,03**	**< 0.0001**
		BD	**27,620**	**0,610**	**99/116**		
	lipl-5(ok3581); oe *lipl-5 (endogenous promoter)*	AL	18,178	0,361	189/193	64,10	< 0.0001
		BD	29,830	0,455	126/144		
	lipl-5(ok3581)	AL	**18,160**	**0,510**	**111/141**	1,38	0.651
	lipl-5(ok3581); oe lipl-5 (endogenous promoter)		**18,410**	**0,400**	**136/141**		
	lipl-5(ok3581)	BD	**31,280**	**0,770**	**67/109**	-11,70	P < 0.001
	lipl-5(ok3581); oe lipl-5 (endogenous promoter)		**27,620**	**0,610**	**99/116**		

Figure 6A	**Wild-type N2**	**AL**	**17,638**	**0,527**	**118/126**	**41,84**	**< 0.0001**
		BD	**25,017**	**0,569**	**95/116**		
	coel.(-)	**AL**	**14,815**	**0,440**	**107/110**	**89,44**	**< 0.0001**
		BD	**28,066**	**0,646**	**89/107**		
	coel.(-)	AL	14,405	0,383	122/123	109,48	< 0.0001
		BD	30,175	0,706	106/130		
	coel.(-)	AL	13,718	0,422	106/120	108,32	< 0.0001
		BD	28,578	0,780	96/126		
	coel.(-)	AL	16,611	0,564	99/118	78,63	< 0.0001
		BD	29,672	0,670	101/144		
	coel.(-)	AL	16,237	0,568	113/116	90,49	< 0.0001
		BD	30,930	0,749	77/134		
	coel.(-)	AL	17,173	0,341	207/218	91,36	< 0.0001
		BD	32,862	0,399	213/231		
	Wild-type N2	AL	**17,638**	**0,527**	**118/126**	-16,01	< 0.001
	coel.(-)		**14,815**	**0,440**	**107/110**		
	Wild-type N2	BD	**25,017**	**0,569**	**95/116**	12,19	< 0.001
	coel.(-)		**28,066**	**0,646**	**89/107**		

Figure 7 B	**coel.(-)**	**AL**	**14,815**	**0,440**	**107/110**	**89,44**	**< 0.0001**
		BD	**28,066**	**0,646**	**89/107**		
	coel.(-);*lipl-5(ok3581)*	AL	12,676	0,449	107/121	154,80	< 0.0001
		BD	32,299	0,528	108/134		
	coel.(-);*lipl-5(ok3581)*	**AL**	**15,266**	**0,522**	**116/123**	**106,20**	**< 0.0001**
		BD	**31,479**	**0,701**	**103/138**		
	coel.(-);*lipl-5(ok3581)*	AL	17,335	0,536	119/130	80,65	< 0.0001
		BD	31,315	0,828	90/147		
	coel.(-);*lipl-5(ok3581)*	AL	17,232	0,387	171/178	87,73	< 0.0001
		BD	32,349	0,480	160/171		
	coel.(-)	**AL**	**14,815**	**0,440**	**107/110**	3,04	0.185
	coel.(-);*lipl-5(ok3581)*		**15,266**	**0,522**	**116/123**		
	coel.(-)	**BD**	**28,066**	**0,646**	**89/107**	12,16	< 0.05
	coel.(-);*lipl-5(ok3581)*		**31,479**	**0,701**	**103/138**		
Figure 7 D	**coel.(-)**	**AL**	**14,815**	**0,440**	**107/110**	**89,44**	**< 0.0001**
		BD	**28,066**	**0,646**	**89/107**		
	coel.(-);oe *lipl-5 (endogenous promoter)*	**AL**	**14,543**	**0,666**	**89/103**	**92,32**	**< 0.0001**
		BD	**27,969**	**0,564**	**124/143**		
	coel.(-);oe *lipl-5 (endogenous promoter)*	AL	15,589	0,479	123/131	75,37	< 0.0001
		BD	27,339	0,679	72/115		
	coel.(-);oe *lipl-5 (endogenous promoter)*	AL	15,436	0,444	122/123	95,45	< 0.0001
		BD	30,170	0,440	101/155		
	coel.(-)	**AL**	**14,815**	**0,440**	**107/110**	-1,84	0.234
	coel.(-);oe *lipl-5 (endogenous promoter)*		**14,543**	**0,666**	**89/103**		
	coel.(-)	**BD**	**28,066**	**0,646**	**89/107**	-0,35	0.309
	coel.(-);oe *lipl-5 (endogenous promoter)*		**27,969**	**0,564**	**124/143**		

Figure S5 C	***lipl-5(ok3581)***	**AL**	**17,987**	**0,388**	**172/183**	**85,45**	**< 0.0001**
		BD	**33,357**	**0,464**	**143/157**		
	lipl-5(ok3581)	AL	23,130	0,480	193/194	32,77	< 0.0001
		BD	30,709	0,429	155/180		
	lipl-5(ok3581)	AL	23,847	0,533	177/179	47,73	< 0.0001
		BD	35,229	0,417	157/184		
	lipl-5(ok3581); oe lipl-5 (pges-1 promoteur)	**AL**	**19,240**	**0,352**	**185/192**	**48,43**	**< 0.0001**
		BD	**28,558**	**0,522**	**142/167**		
	lipl-5(ok3581); oe lipl-5 (pges-1 promoteur)	AL	24,192	0,413	205/210	19,56	< 0.0001
		BD	28,925	0,461	165/176		
	lipl-5(ok3581); oe lipl-5 (pges-1 promoteur)	AL	23,643	0,521	182/183	37,41	< 0.0001
		BD	32,487	0,562	144/189		
	lipl-5(ok3581)	**AL**	**17,987**	**0,388**	**172/183**	6,97	< 0.05
	lipl-5(ok3581); oe lipl-5 (pges-1 promoteur)		**19,240**	**0,352**	**185/192**		
	lipl-5(ok3581)	**BD**	**33,357**	**0,464**	**143/157**	-14,39	< 0.001
	lipl-5(ok3581); oe lipl-5 (pges-1 promoteur)		**28,558**	**0,522**	**142/167**		

Table S2: Lifespan data, Related to Figures 1, 4, 6, 7, 8 and S5

Lifespan data corresponding to lifespan curves shown in the figures appear in bold in the table.

	Forward	Reverse
Plasmid pAB01 construction	SalI/lipl-5 F: 5′-CTGGTCGACATGTGGC GGTTTGCCGTTTTTC-3′	lipl-5/KpnI R: 5′-GTGGTACCTTTCCCAAATAATCGT CAG TGCACAGC-3′
Plasmid pAB02 construction	lipl-5p/lipl-5 gibson F: 5′-CAC AAC GAT GGA TAC GCT AAC AAC TTG GAA ATG AAA TAA GCT TCT AAA ACA ATT ATT TTC AGA CGA TAC TTG GTC-3′	lipl-5p/lipl-5 gibson R: 5′-GAT GAC CTC CTC GCC CTT GCT CAC CAT TAC CGG TAC CGA TTT TCC CAA ATA ATC GTC AGT GC-3′
Plasmid pAB03 construction: primers PCR1	F1 (Plasmid+Pcc1): 5′-CGC TAA CAA CTT GGA AAT GAA ATA AGC TTG TTG ACA CGC AGT TTC CCT-3′	R1F2 (Pcc1+lipl-5): 5′-AAC GGC AAA CCG CCA CAT ATT GTG AGC CCA ATG AAG TAA AAT TTC-3′
Plasmid pAB03 construction: primers PCR2	R1F2 (Pcc1+lipl-5): 5′-GAA ATT TTA CTT CAT TGG GCT CAC AAT ATG TGG CGG TTT GCC GTT-3′	R2 (lipl-5+Plasmid): 5′-CCC TTG CTC ACC ATT ACC GGT ACC GAT TTT CCC AAA TAA TCG TCA GTG CAC-3′
RT-qPCR primer PMP-3	5’-GTT CCC GTG TTC ATC ACT CAT-3′	5′-ACA CCG TCC AGA AGC TGT AGA-3′
RT-qPCR primer CDC-42	5′-CTG CTG GAC AGG AAG ATT ACG-3′	5′-CTC GGA CAT TCT CGA ATG AAG-3′
RT-qPCR primer ACT-1	5′-GCT GGA CGT GAT CTT ACT GAT TAC C-3′	5′-GTA GCA GAG CTT CTC CTT GAT GTC-3′
RT-qPCR primer LILP-1	5′-CGG TTT GCG CTG GAC TTA-3′	5′-GAA CAC GAG TTG CGT TAA-3′
RT-qPCR primer LIPL-2	5′-TGG ATG CAG ATG GTT CGC AA-3′	5′-GCC CTT GAT GGC TCC GAA AT-3′
RT-qPCR primer LIPL-3	5′-GCT CGT GAT TCT TGC GGT TC-3′	5′-CGG ATA ACC CCA TCG CTC AA-3′
RT-qPCR primer LIPL-4	5′-GAA ACG TTG TTC GCG CAG TT-3′	5′-AAC TTG GCT GGC TGC ATT TG-3′
RT-qPCR primer LIPL-5	5′-ACT GGG GAA CCA AGA CGA AC-3′	5′-TAT CAG CCA ACC AAT CGG CA-3′

Table S3: Oligonucleotide information, Related to Figures 2, 3, 4, 5, 6, 7, S3 and S7.